

# The WNK-regulated SPAK/OSR1 kinases directly phosphorylate and inhibit the $K^+ - Cl^-$ co-transporters

Paola DE LOS HEROS\*, Dario R. ALESSI\*<sup>1</sup>, Robert GOURLAY\*, David G. CAMPBELL\*, Maria DEAK\*, Thomas J. MACARTNEY\*, Kristopher T. KAHLE†‡ and Jinwei ZHANG\*<sup>1</sup>

\*MRC Protein Phosphorylation and Ubiquitylation Unit, College of Life Sciences, University of Dundee, Dow Street, Dundee DD1 5EH, Scotland, U.K.

†Department of Neurosurgery, Massachusetts General Hospital, and Harvard Medical School, Boston, MA 02114, U.S.A.

‡Manton Center for Orphan Disease Research, Children's Hospital Boston, Boston, MA 02115, U.S.A.

Precise homeostasis of the intracellular concentration of  $Cl^-$  is achieved via the co-ordinated activities of the  $Cl^-$  influx and efflux. We demonstrate that the WNK (WNK lysine-deficient protein kinase)-activated SPAK (SPS1-related proline/alanine-rich kinase)/OSR1 (oxidative stress-responsive kinase 1) known to directly phosphorylate and stimulate the N[K]CCs ( $Na^+ - K^+$  ion co-transporters), also promote inhibition of the KCCs ( $K^+ - Cl^-$  co-transporters) by directly phosphorylating a recently described C-terminal threonine residue conserved in all KCC isoforms [Site-2 (Thr<sup>1048</sup>)]. First, we demonstrate that SPAK and OSR1, in the presence of the MO25 regulatory subunit, robustly phosphorylates all KCC isoforms at Site-2 *in vitro*. Secondly, STOCK1S-50699, a WNK pathway inhibitor, suppresses SPAK/OSR1 activation and KCC3A Site-2 phosphorylation with similar efficiency. Thirdly, in ES (embryonic stem) cells lacking SPAK/OSR1 activity, endogenous phosphorylation of KCC isoforms at Site-2 is abolished and these cells display elevated basal activity of <sup>86</sup>Rb<sup>+</sup> uptake that was not markedly stimulated further by hypotonic high  $K^+$  conditions, consistent with KCC3A activation. Fourthly, a tight correlation exists between SPAK/OSR1 activity and the magnitude of KCC3A Site-2 phosphorylation. Lastly, a Site-2 alanine KCC3A mutant

preventing SPAK/OSR1 phosphorylation exhibits increased activity. We also observe that KCCs are directly phosphorylated by SPAK/OSR1, at a novel Site-3 (Thr<sup>5</sup> in KCC1/KCC3 and Thr<sup>6</sup> in KCC2/KCC4), and a previously recognized KCC3-specific residue, Site-4 (Ser<sup>96</sup>). These data demonstrate that the WNK-regulated SPAK/OSR1 kinases directly phosphorylate the N[K]CCs and KCCs, promoting their stimulation and inhibition respectively. Given these reciprocal actions with anticipated net effects of increasing  $Cl^-$  influx, we propose that the targeting of WNK-SPAK/OSR1 with kinase inhibitors might be a novel potent strategy to enhance cellular  $Cl^-$  extrusion, with potential implications for the therapeutic modulation of epithelial and neuronal ion transport in human disease states.

**Key words:**  $\gamma$ -aminobutyric acid (GABA), blood pressure/hypertension, ion homeostasis,  $K^+ - Cl^-$  co-transporter 2 (KCC2),  $K^+ - Cl^-$  co-transporter 3 (KCC3),  $Na^+ - Cl^-$  co-transporter (NCC),  $Na^+ - K^+ - 2Cl^-$  co-transporter 1 (NKCC1), protein kinase, signal transduction.

## INTRODUCTION

In eukaryotic cells, the regulation of intracellular  $Cl^-$  concentration ( $[Cl^-]_i$ ) is important for multiple essential cellular processes, including cell volume homeostasis, which counters excessive shrinkage or swelling amidst changes in extracellular tonicity and/or intracellular ion content [1]. The *SLC12A* (solute carrier family 12) family of electroneutral CCCs (cation- $Cl^-$  co-transporters), by transporting  $Cl^-$  against or with its electrochemical gradient, are critical determinants of  $[Cl^-]_i$  [2].  $Cl^-$  influx is powered by the  $Na^+$ -driven CCC members, which includes the NCC ( $Na^+ - Cl^-$  co-transporter) in the distal convoluted tubule of the kidney [3,4], the NKCC2 ( $Na^+ - K^+ - 2Cl^-$  co-transporter 2) in the thick ascending limb of the kidney [5] and the ubiquitously expressed NKCC1 [6–8].  $Cl^-$  efflux is powered by the  $K^+$ -driven CCCs, which include four different  $K^+ - Cl^-$  co-transporters (KCC1–KCC4) [9], including the neuron-specific KCC2. There are two well-studied splice variants of KCC2, termed KCC2 and KCC2A [10], and of KCC3, termed KCC3 and KCC3A [11]. The physiological importance of the CCCs is illustrated by the human

Mendelian diseases or mouse phenotypes that result from their mutation or dysfunction [12], and that two CCCs are the targets of the most commonly used drugs in medicine, the loop-diuretic furosemide (inhibiting NKCC2) and thiazide diuretics (inhibiting NCC) [13]. The activities of the NCC/NKCC1/NKCC2 (i.e. N[K]CCs [ $Na^+ - K^+$  ion co-transporters]) and KCCs are reciprocally regulated by protein (de)phosphorylation [9,14,15]. Phosphorylation activates NCC/NKCC1/NKCC2, but inhibits KCCs [9,15–17]. Dephosphorylation has the opposite effect. This reciprocal regulation of  $Na^+$ - and  $K^+$ -driven CCCs ensures that cellular  $Cl^-$  influx and efflux is tightly co-ordinated [9,18]. The importance of this mechanism is exemplified by its evolutionary conservation from worms to humans [19].

Experiments have defined the WNK (WNK lysine-deficient protein kinase) serine/threonine kinases [20] and their downstream kinase substrates SPAK [SPS1-related proline/alanine rich kinase; also known as STK39 (serine/threonine kinase 39)]/OSR1 (oxidative stress-responsive kinase 1) [21] as the essential phospho-regulators that stimulate N[K]CC activity. WNK isoforms activate the two highly related SPAK and OSR1

Abbreviations: CCC, cation- $Cl^-$  co-transporter; CCT, conserved C-terminal; CTD, C-terminal cytoplasmic domain; ERK1, extracellular-signal-regulated kinase 1; ES, embryonic stem; HEK, human embryonic kidney; HRP, horseradish peroxidase; KCC,  $K^+ - Cl^-$  co-transporter; LDS, lithium dodecyl sulfate; NCC,  $Na^+ - Cl^-$  co-transporter; N[K]CC,  $Na^+ - K^+$  ion co-transporter; NKCC,  $Na^+ - K^+ - 2Cl^-$  co-transporter; NTD, N-terminal cytoplasmic domain; OSR1, oxidative stress-responsive kinase 1; SLC12, solute carrier family 12; SPAK, SPS1-related proline/alanine-rich kinase; TTBS, Tris-buffered saline containing Tween 20; WNK, WNK lysine-deficient protein kinase; XIC, extracted ion chromatogram.

<sup>1</sup> Correspondence may be addressed to either of these authors (email d.r.alessi@dundee.ac.uk or j.c.zhang@dundee.ac.uk).

proteins [22] by phosphorylating a critical threonine residue (SPAK Thr<sup>233</sup> and OSR1 Thr<sup>185</sup>) within their catalytic T-loop motif [23,24]. SPAK and OSR1 also interact with the scaffolding protein MO25 [also known as CAB39 (Ca<sup>2+</sup>-binding protein 39)] that enhances their catalytic activity over 100-fold [25]. SPAK and OSR1 bind NCC, NKCC1 and NKCC2 via a unique CCT (conserved C-terminal) docking domain that recognizes highly conserved RFXV/I motifs at the N-terminal domain of these CCCs [4–6,26–28]. The CCT domain also plays a critical role in enabling SPAK/OSR1 to be activated by interacting with RFXV/I motifs on WNK isoforms [24,26,29]. Recently, an inhibitor (STOCK1S-50699) that interacts with the CCT domain of SPAK and OSR1 and consequently prevents their activation by WNK kinases has been shown to potently suppress SPAK/OSR1 activity and NCC/NKCC1 phosphorylation [30]. WNK isoforms, and hence SPAK/OSR1, are activated rapidly following hypertonic or hypotonic low Cl<sup>-</sup> conditions [3,24,31]. Following activation, SPAK/OSR1 phosphorylate a cluster of conserved threonine residues in the NTD (N-terminal cytoplasmic domain) of the N[K]CCs [25].

In the kidney, the WNK–SPAK/OSR1-mediated activation of NCC and NKCC2, which together mediate ~25% of renal salt reabsorption, is critical for extracellular volume (influencing blood pressure) and electrolyte homeostasis. The importance of this pathway in human renal physiology is underscored by the findings that: (i) gain-of-function mutations in WNK1 and WNK4 resulting in increased NCC and NKCC2 activities cause a Mendelian syndrome featuring thiazide-sensitive hypertension and hyperkalaemia (pseudohypoaldosteronism type II, also known as PHAII [32]); (ii) loss-of-function mutations in NCC [33] and NKCC2 [34] cause Gitelman's and Bartter's type 1 syndromes respectively, featuring hypotension and hypokalaemia; and (iii) a mutation of NCC at a residue (T60M) that ablates the key activating WNK-regulated SPAK/OSR1 phosphorylation event causes Gitelman's syndrome in Asian people [35]. Moreover, SPAK-knockout mice [36], or knockin mice expressing a form of SPAK or OSR1 that cannot be activated by WNK kinase isoforms [37], exhibit low blood pressure and are resistant to hypertension when crossed to animals bearing a PHAII-causing knockin mutation that enhances WNK4 expression [38].

In contrast with the N[K]CCs, the direct mediators of KCC phospho-regulation are not known, although early experiments suggested the WNK–SPAK/OSR1 kinases may be involved [39–41]. Work to date indicates that two threonine residues that are conserved in all KCC isoforms, termed Site-1 (Thr<sup>991</sup> in KCC3) and Site-2 (Thr<sup>1048</sup> in KCC3), both located within the CTD (C-terminal cytoplasmic domain), play a critical role in controlling the activity of the KCCs [42]. Hypotonic high K<sup>+</sup> conditions that activate KCC isoforms induce a rapid and robust dephosphorylation of Site-1 and Site-2 [42]. Consistent with these sites representing critical regulatory residues, mutation of Site-1 and Site-2 to alanine in KCC3 results in a constitutively active co-transporter [42]. The identity of the protein kinases that phosphorylate Site-1 and Site-2, however, are currently unknown, although the WNK1 signalling pathway has been implicated, as siRNA-mediated knockdown of WNK1 partially suppressed the phosphorylation of these residues in KCC3 [42]. Consistent with a role for WNK isoforms in controlling KCC activity, overexpression of WNK3 and WNK4 in oocytes and mammalian cells leads to the inhibition of KCC isoforms, and kinase-dead overexpression of WNK3 was found to potently stimulate KCC activity [39,40,43–45].

In the present study, we explore the mechanism by which WNKs might regulate KCC phosphorylation. Our data reveal for the first time that the WNK-controlled SPAK/OSR1 act as

direct phosphorylators and major regulators of the KCC isoforms, and explain how activation of the WNK signalling pathway can co-ordinately regulate Cl<sup>-</sup> influx and efflux by reciprocally controlling the SLC12 family N[K]CC and KCC isoforms. Given these reciprocal actions with anticipated net effects of increasing Cl<sup>-</sup> influx, we propose that inhibition of the WNK–SPAK/OSR1 signalling pathway might be a potent strategy to enhance cellular Cl<sup>-</sup> extrusion, with potential therapeutic implications.

## MATERIALS AND METHODS

### Antibodies

The following antibodies were raised in sheep and affinity-purified on the appropriate antigen by the Division of Signal Transduction Therapy Unit at the University of Dundee: anti-KCC1 total antibody (residues 1–118 of human KCC1), anti-KCC2A total antibody (residues 1–119 of human KCC2A), anti-KCC3A total antibody (residues 1–175 of human KCC3A), anti-KCC4 total antibody (residues 1–117 of human KCC4), anti-KCC3A phospho-Ser<sup>96</sup> antibody [residues 89–103 of human KCC3A phosphorylated at Ser<sup>96</sup>; IEDLSQN(S)ITGEHSQ], anti-KCC3A phospho-Thr<sup>991</sup> [residues 984–998 of human KCC3A phosphorylated at Thr<sup>991</sup>; SAYTYER(T)LMMEQRSRR], anti-KCC3A phospho-Thr<sup>1048</sup> (residues 1041–1055 of human KCC3A phosphorylated at Thr<sup>1048</sup>; CYQEKVHM(T)WTKDKYM), anti-NKCC1 total antibody (residues 1–288 of human NKCC1), anti-NKCC1 phospho-Thr<sup>203</sup>/Thr<sup>207</sup>/Thr<sup>212</sup> antibody [residues 198–217 of human NKCC1 phosphorylated at Thr<sup>203</sup>, Thr<sup>207</sup> and Thr<sup>212</sup>; HYYYD(T)HTN(T)YYLR(T)FGHNT], anti-WNK1 total antibody (residues 2360–2382 of human WNK1), anti-WNK1 phospho-Ser<sup>382</sup> antibody [residues 377–387 of human WNK1 phosphorylated at Ser<sup>382</sup>; ASFAK(S)VIGTP]; anti-SPAK total antibody (full-length GST-tagged human SPAK protein), anti-SPAK/OSR1 (S-motif) phospho-Ser<sup>373</sup>/Ser<sup>325</sup> antibody [residues 367–379 of human SPAK; RRVPGS(S)GHLHKT; highly similar to residues 319–331 of human OSR1 in which the sequence is RRVPGS(S)GRLHKT] and anti-ERK1 (extracellular-signal-regulated kinase 1) total antibody (full-length human ERK1 protein). The anti-FLAG antibody (catalogue number F1804) was purchased from Sigma–Aldrich. Secondary antibodies coupled to HRP (horseradish peroxidase) used for immunoblotting were obtained from Pierce. IgG used in control immunoprecipitation experiments was affinity-purified from pre-immune serum using Protein G–Sepharose.

### Buffers

Buffer A contained 50 mM Tris/HCl (pH 7.5) and 0.1 mM EGTA. Lysis buffer was 50 mM Tris/HCl (pH 7.5), 1 mM EGTA, 1 mM EDTA, 50 mM sodium fluoride, 5 mM sodium pyrophosphate, 1 mM sodium orthovanadate, 1% (w/v) Nonidet P40, 0.27 M sucrose, 0.1% 2-mercaptoethanol and protease inhibitors (1 tablet per 50 ml). TTBS (Tris-buffered saline containing Tween 20) was Tris/HCl (pH 7.5), 0.15 M NaCl and 0.2% Tween 20. SDS sample buffer was 1 × NuPAGE LDS sample buffer (Invitrogen), containing 1% (v/v) 2-mercaptoethanol. Isotonic high potassium buffer was 95 mM NaCl, 50 mM KCl, 1 mM CaCl<sub>2</sub>, 1 mM MgCl<sub>2</sub>, 1 mM Na<sub>2</sub>HPO<sub>4</sub>, 1 mM Na<sub>2</sub>SO<sub>4</sub> and 20 mM Hepes (pH 7.4). Hypotonic high potassium buffer was 80 mM KCl, 1 mM CaCl<sub>2</sub>, 1 mM MgCl<sub>2</sub>, 1 mM Na<sub>2</sub>HPO<sub>4</sub>, 1 mM Na<sub>2</sub>SO<sub>4</sub> and 20 mM Hepes (pH 7.4). Isotonic buffer was 135 mM NaCl, 5 mM KCl, 0.5 mM CaCl<sub>2</sub>, 0.5 mM MgCl<sub>2</sub>, 0.5 mM Na<sub>2</sub>HPO<sub>4</sub>, 0.5 mM Na<sub>2</sub>SO<sub>4</sub> and 15 mM Hepes (pH 7.5). Hypotonic low chloride buffer

was 67.5 mM sodium gluconate, 2.5 mM potassium gluconate, 0.25 mM CaCl<sub>2</sub>, 0.25 mM MgCl<sub>2</sub>, 0.5 mM Na<sub>2</sub>HPO<sub>4</sub>, 0.5 mM Na<sub>2</sub>SO<sub>4</sub> and 7.5 mM Hepes (pH 7.5).

### Plasmids

Full-length human KCCs isoforms were amplified employing SuperScript III (Invitrogen) from placenta total RNA (Stratagene) using the appropriate oligonucleotides. The RT-PCR (reverse transcription-PCR) products were ligated into the pCR2.1-TOPO vector and sequenced. The sequence-verified KCCs were subcloned into bacterial (pGEX-6P-1) and mammalian (pCMV5) expression vectors using BamHI and NotI. Required amino acid mutations were introduced into the pCR2.1-TOPO clone using site-directed mutagenesis by QuikChange method (Stratagene), but substituting the Taq enzyme with KOD Hot Start DNA polymerase (Novagen). Oligonucleotides were obtained from Invitrogen Life Sciences. DNA sequencing was performed by The Sequencing Service, College of Life Sciences, University of Dundee (<http://www.dnaseq.co.uk>).

### Cell culture, transfections and stimulations

HEK (human embryonic kidney)-293 cells were cultured on 10-cm-diameter dishes in DMEM (Dulbecco's modified Eagle's medium) supplemented with 10% (v/v) FBS, 2 mM L-glutamine, 100 units/ml penicillin and 0.1 mg/ml streptomycin. For transfection experiments, each dish of adherent HEK-293 cells was transfected with 20  $\mu$ l of 1 mg/ml polyethylenimine (Polysciences) and 5–10  $\mu$ g of plasmid DNA as described previously [46]. At 36 h post-transfection cells were stimulated with either control isotonic or hypotonic medium for a period of 30 min. Cells were lysed in 0.3 ml of ice-cold lysis buffer/dish, lysates were clarified by centrifugation at 4°C for 15 min at 26000 g and the supernatants were frozen in aliquots in liquid nitrogen and stored at -20°C. Protein concentrations were determined using the Bradford method. Where indicated cells were treated with the indicated concentrations of the SPAK/OSR1 CCT domain inhibitor STOCK1S-50699 [30], which was purchased from InterBioScreen.

### Expression and purification of OSR1 T185E and D164A, SPAK D212A, and KCCs N-terminal and C-terminal domains in *Escherichia coli* cells

All pGEX-6P-1 constructs were transformed into BL21 *E. coli* cells and 1-litre cultures were grown at 37°C in LB broth containing 100  $\mu$ g/ml ampicillin until the attenuation at 600 nm was 0.8. IPTG (30  $\mu$ M) was then added and the cells were cultured for a further 16 h at 26°C. Cells were isolated by centrifugation (4°C for 30 min at 3500 g), resuspended in 40 ml of ice-cold lysis buffer and lysed in one round of freeze-thawing, followed by sonication (Branson Digital Sonifier; ten 15-s pulses with a setting of 45% amplitude) to fragment DNA. Lysates were centrifuged at 4°C for 15 min at 26000 g. The GST-fusion proteins were affinity-purified on 0.5 ml of glutathione-Sepharose and eluted in buffer A containing 0.27 M sucrose and 20 mM glutathione.

### Immunoblotting and phospho-antibody immunoprecipitation

Cell lysates (15  $\mu$ g) in SDS sample buffer were subjected to electrophoresis on polyacrylamide gels and transferred on to nitrocellulose membranes. The membranes were incubated for 30 min with TTBS containing 5% (w/v) non-fat powdered skimmed milk. The membranes were then immunoblotted in 5%

(w/v) non-fat powdered skimmed milk in TTBS with the indicated primary antibodies overnight at 4°C. Sheep antibodies were used at a concentration of 1–2  $\mu$ g/ml. The incubation with phospho-specific sheep antibodies was performed with the addition of 10  $\mu$ g/ml of the dephospho-peptide antigen used to raise the antibody. The blots were then washed six times with TTBS and incubated for 1 hour at room temperature (15–20°C) with secondary HRP-conjugated antibodies diluted 5000-fold in 5% (w/v) non-fat powdered skimmed milk in TTBS. After repeating the washing steps, the signal was detected using an ECL reagent. Immunoblots were developed using a film automatic processor (SRX-101; Konica Minolta Medical) and films were scanned with a 600 d.p.i. resolution on a scanner (PowerLook 1000; UMAX). Figures were generated using Photoshop/Illustrator (Adobe). For phospho-antibody immunoprecipitation, KCC isoforms were immunoprecipitated from indicated cell extracts. An aliquot (2 mg) of the indicated clarified cell extract was incubated with 15  $\mu$ g of the indicated phospho-specific KCC antibody conjugated to 15  $\mu$ l of Protein G-Sepharose in the presence of 20  $\mu$ g of the dephosphorylated peptide encompassing the residues on KCC that the antibody was raised against. Incubation was for 2 h at 4°C with gentle agitation, and the immunoprecipitates were washed three times with 1 ml of lysis buffer containing 0.15 M NaCl and twice with 1 ml of buffer A. Bound proteins were eluted with 1  $\times$  LDS sample buffer.

### Mapping phosphorylation sites of KCCs by active SPAK

KCC1 (residues 1–118), KCC1 (residues 872–1085), KCC2A (residues 1–119), KCC2A (residues 852–1039), KCC3A (residues 1–117), KCC3A (residues 886–1141), KCC4 (residues 1–174) and KCC4 (residues 872–1083) (10  $\mu$ g of each) purified from *E. coli* cells were incubated with active SPAK [Carna Biosciences STLK3 (STK39); product number 07-130] (0.5  $\mu$ g) or kinase-inactive SPAK-SPAK [D212A] (0.5  $\mu$ g) also purified from *E. coli* cells, at 30°C for 60 min in buffer A containing 10 mM MgCl<sub>2</sub>, 0.1 mM [ $\gamma$ -<sup>32</sup>P]ATP (approximately 15000 c.p.m./pmol) in a total reaction volume of 25  $\mu$ l. The reaction was terminated by the addition of LDS sample buffer. DTT was added to a final concentration of 10 mM, the samples heated at 95°C for 5 min and cooled for 20 min at room temperature. Iodoacetamide was then added to a final concentration of 50 mM and the samples left in the dark for 30 min at room temperature to alkylate the cysteine residues. The samples were subjected to electrophoresis on a Bis-Tris 10% polyacrylamide gel, which was stained with Colloidal Blue and then autoradiographed. The corresponding phosphorylated bands were excised, cut into smaller pieces and washed sequentially for 10 min on a vibrating platform with 1 ml of each of the following: water, 1:1 (v/v) mixture of water and acetonitrile, 0.1 M ammonium bicarbonate, 1:1 mixture of 0.1 M ammonium bicarbonate and acetonitrile, and finally acetonitrile. The gel pieces were dried before incubation for 16 h at 30°C in 25 mM triethylammonium bicarbonate containing 5  $\mu$ g/ml trypsin as described previously [47]. Following tryptic digestion, >95% of the <sup>32</sup>P radioactivity incorporated in the gel bands was recovered and the samples were chromatographed on a Vydac 218TP5215 C<sub>18</sub> column (Separations Group) equilibrated in 0.1% trifluoroacetic acid in water. The column was developed with a linear acetonitrile gradient at a flow rate of 0.2 ml/min and fractions of 0.1 ml were collected. Some phosphopeptide fractions (Tables 1 and 2) were purified further by immobilized metal-chelate affinity chromatography on Phos-Select resin (Sigma) as described previously [48].

**Table 1 SPAK in the presence of MO25 phosphorylates KCC isoforms at two conserved Site-2 and Site-3 residues**

The NTD and CTD of the indicated KCC isoforms were phosphorylated by SPAK (except for <sup>32</sup>P cycle release data indicated with an asterisk that was phosphorylated by OSR1) in the presence of MO25 with either radioactive [ $\gamma$ -<sup>32</sup>P]ATP or non-radioactive Mg-ATP. Phosphorylated fragments were trypsin digested and the resulting tryptic peptides were isolated by HPLC for the <sup>32</sup>P-labelled ones. The identity and site of phosphorylation was determined by a combination of MS and solid-phase Edman sequencing. Non-radioactive KCC fragments phosphorylated by SPAK were analysed by orbitrap MS. The deduced amino acid sequence of each peptide is shown and the phosphorylated residue is underlined and in bold font. The resultant data was searched using the Mascot search algorithm (<http://www.matrixscience.com>) run on a local server. For conservation and location of sites see Figure 2. It should be noted that although experiments were done with the shorter KCC3A splice variant that lacks nine N-terminal residues, in order to be consistent with most previous literature studies, numbering of residues is based on the nine-residue-longer KCC3 variant.

Sample	Phosphopeptide	<sup>32</sup> P HPLC Edman sequencing		MS (orbitrap)		
		Mascot score	Cycle of <sup>32</sup> P release	Mascot score	<i>m/z</i> (observed)	Phosphorylation site
NTD (KCC1)	SDLEVLFGQLGSGTSMPHF <b>I</b> VVPVDGPR	90*	20*	82	1531.75	Thr <sup>5</sup> (Site-3)
CTD (KCC1)	IQMTWTR	27	4	26	508.22	Thr <sup>983</sup> (Site-2)
NTD (KCC2A)	RFT <b>I</b> VTSLPPAGPAR	61	3	66	775.39	Thr <sup>6</sup> (Site-3)
CTD (KCC2A)	VH <b>L</b> TWTK	Not detected	Not detected	20	482.73	Thr <sup>1030</sup> (Site-2)
NTD (KCC3A)	TSH <b>P</b> QDVIEDLSQ <b>N</b> SITGEHSQLLDDG <b>H</b> K	53	15	55	1094.16	Ser <sup>96</sup> (Site-4)
CTD (KCC3A)	VH <b>M</b> <b>I</b> TWTK	Not detected	Not detected	6	491.71	Thr <sup>1048</sup> (Site-2)
CTD (KCC4)	VQ <b>M</b> <b>I</b> TWTR	Not detected	Not detected	40	501.21	Thr <sup>980</sup> (Site-2)

**Table 2 Summary of other *in vitro* SPAK phosphorylation sites that were identified, but not investigated further in the present study**

Analysis was undertaken as described in the legend of Table 1. For conservation and location of these sites see Figure 2. Peptides with a *m/z* (observed) marked with 1P correspond to peptide mass with one phosphate and those with 2P correspond to a peptide with two phosphates. Phosphorylated residues are underlined and in bold font. Lower case m indicates oxidized methionine.

Sample	Phosphopeptide	<sup>32</sup> P HPLC Edman sequencing		MS (orbitrap)		
		Mascot score	Cycle of <sup>32</sup> P release	Mascot score	<i>m/z</i> (observed)	Phosphorylation site(s)
CTD (KCC1)	DKY <b>M</b> <b>I</b> TETWDPSPHADPNFR	Not performed	Not performed	41	763.98	Thr <sup>991</sup> or Thr <sup>993</sup>
NTD (KCC2A)	NmALFEEEmDT <b>S</b> PmV <b>S</b> LLSGLANY <b>T</b> NLPQGS <b>R</b>	43	12 or 26	Not performed	933.41 (1P)	Ser <sup>83</sup> or Thr <sup>92</sup>
	NmALFEEEmDT <b>S</b> PmV <b>S</b> LLSGLANY <b>T</b> NLPQGS <b>R</b>	65	11, 12, 17 and 26	Not performed	1244.21 (1P)	Thr <sup>77</sup> and/or Ser <sup>78</sup> , and/or Ser <sup>83</sup> and/or Thr <sup>92</sup>
	NmALFEEEmDT <b>S</b> PmV <b>S</b> LLSGLANY <b>T</b> NLPQGS <b>R</b>	42	11, 12, 17 and 26	Not performed	1270.87 (2P)	Thr <sup>77</sup> and/or Ser <sup>78</sup> , and/or Ser <sup>83</sup> and/or Thr <sup>92</sup>
NTD (KCC3A)	mANY <b>T</b> N <b>L</b> I <b>Q</b> GAKEHEEAENITE <b>G</b> K	Not performed	Not performed	57	925.40	Thr <sup>160</sup>
	FMV <b>T</b> PTKID <b>I</b> D <b>I</b> PLG <b>S</b> DT <b>S</b> PD <b>L</b> SS <b>R</b>	Not performed	Not performed	25	891.42	Ser <sup>32</sup>
CTD (KCC4)	TQAP <b>P</b> <b>T</b> PKV <b>Q</b> M <b>T</b> W <b>T</b> R	Not performed	Not performed	25	646.30	Thr <sup>973</sup>
	TQAP <b>P</b> TP <b>D</b> K <b>V</b> Q <b>M</b> <b>I</b> W <b>T</b> R	Not performed	Not performed	24	968.95	Thr <sup>980</sup> (Site-2) or Thr <sup>982</sup>

## MS analysis

Isolated phosphopeptides were analysed by MS analysis as follows. LC-MS/MS was performed using a linear ion trap-orbitrap hybrid mass spectrometer (Orbitrap Classic; Thermo Fisher Scientific) equipped with a nano-electrospray ion source (Proxeon Biosystems or Thermo) and coupled to a Proxeon EASY-nLC system. Peptides were typically injected on to a Thermo/Dionex (part number 160321) Acclaim PepMap100 reverse-phase C<sub>18</sub> 3  $\mu$ m column, 75  $\mu$ m  $\times$  15 cm, with a flow of 300 nl/min and eluted with a 40 min linear gradient of 95% solvent A (2% acetonitrile and 0.1% formic acid in H<sub>2</sub>O) to 50% solvent B (90% acetonitrile and 0.08% formic acid in H<sub>2</sub>O). The instrument was operated with the 'lock mass' option to improve the mass accuracy of precursor ions and data were acquired in the data-dependent mode, automatically switching between MS and MS/MS acquisition. Full scan spectra (*m/z* 300–1800) were acquired in the orbitrap with resolution  $R = 60\,000$  at *m/z* 400 (after accumulation to a target value of 500\,000). The five most intense ions, above a specified minimum signal threshold, based upon a low resolution ( $R = 15\,000$ ) preview of the survey scan, were fragmented by collision induced dissociation and recorded in the linear ion trap (target value of 20\,000). Multi-stage-activation was used to provide an MS<sup>3</sup> scan of parent ions showing a neutral loss of 48.9885, 32.6570 and 24.4942, allowing for 2<sup>+</sup>, 3<sup>+</sup> and 4<sup>+</sup> ions respectively. The resulting MS<sup>3</sup> scan was automatically combined with the relevant MS/MS scan before data analysis using the Mascot search algorithm (<http://www.matrixscience.com>) run on a local server.

## <sup>32</sup>P-labelled phosphopeptide sequence analysis

The site of phosphorylation of the <sup>32</sup>P-labelled peptides was determined by solid-phase Edman degradation, on an Applied Biosystems 494C sequencer, of the peptide coupled to Sequelon-AA membrane (Applied Biosystems) as described previously [49].

## KCC3A phosphorylation sites *in vivo* identification

Fifteen 10-cm diameter dishes of HEK-293 cells were transfected with 5–10  $\mu$ g of the pCMV5 construct encoding human FLAG-KCC3A using the polyethylenimine method [46]. The cells were cultured for a further 36 h, treated with either basic or hypotonic medium, and lysed in 0.3 ml of ice-cold lysis buffer. The pooled lysate was clarified by centrifugation at 4°C for 10 min at 26\,000 g. FLAG-KCC3A was affinity-purified by incubating 50  $\mu$ l of FLAG-agarose beads with 10 mg of the clarified lysate for 2 h at 4°C. The immunoprecipitates were washed four times with 1 ml of lysis buffer containing 0.15 M NaCl and twice with 1 ml of buffer A. Proteins were eluted from the FLAG beads by the addition of 25  $\mu$ l of 1 $\times$  NuPAGE LDS (lithium dodecyl sulfate) sample buffer to the beads. Eluted proteins were reduced by the addition of 10 mM DTT and were prepared as described above. For the identification of phosphorylation sites, the tryptic digests were analysed by LC-MS on an Applied Biosystems 4000 QTRAP system with precursor ion scanning as described previously [50]. The resultant data were searched using the Mascot search algorithm run on a local server. Tryptic phosphopeptides

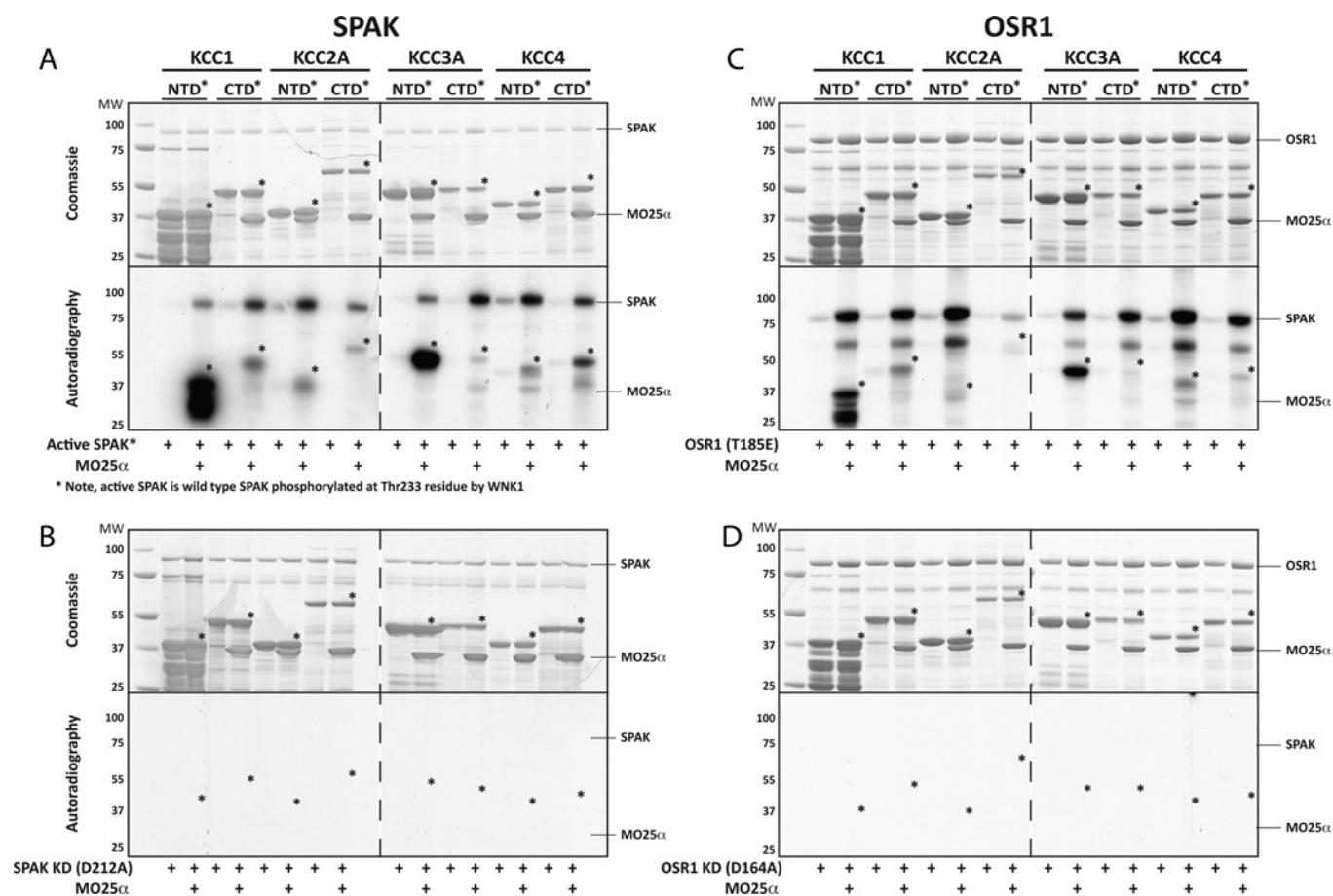


**Figure 1** SPAK and OSR1, complexed to MO25 $\alpha$ , directly phosphorylate KCC isoforms

The NTD and CTD of KCC1 (residues 1–118 and 872–1085 respectively), KCC2A (residues 1–119 and 852–1039 respectively), KCC3A (residues 1–175 and 886–1141 respectively), and KCC4 (residues 1–174 and 872–1083 respectively) were expressed in *E. coli* cells and incubated with an active SPAK purchased from Carna Biosciences which is co-expressed with WNK1 in Sf9 insect cells and hence phosphorylated at Thr<sup>233</sup> and therefore active (A) and OSR1 [T185E] (B), as well as the kinase-inactive (KI) forms of SPAK [D212A] (C) and OSR1 [D164A] (D) in the absence or presence of a 10-molar excess of MO25 $\alpha$ . Reactions were performed in the presence of Mg- $[\gamma\text{-}^{32}\text{P}]\text{ATP}$  for 60 min. Phosphorylation of substrates was analysed following electrophoresis of the Coomassie Blue-stained bands (upper panels) and autoradiography (lower panels). Similar results were obtained in two separate experiments. Broken lines between autoradiographs and gels indicate that the samples were run on separate gels. The bands corresponding to the NTD and CTD fragments are indicated by an asterisk. MW indicates the molecular mass (in kDa).

were also analysed as above under MS analysis and XICs (extracted ion chromatograms) of the isolated phosphopeptides were obtained from the MS RAW data files and analysed with Thermo Scientific<sup>TM</sup> Xcalibur software Version 2.2. Observed variations in charge states, oxidation states and partial cleavages were taken into account when calculating the total XIC for a particular phosphorylation site. The mass range used for the XICs was the observed  $m/z$  value  $\pm$  10 p.p.m. of the relevant peptide.

#### <sup>86</sup>Rb<sup>+</sup>-uptake assay in ES and HEK-293 cells

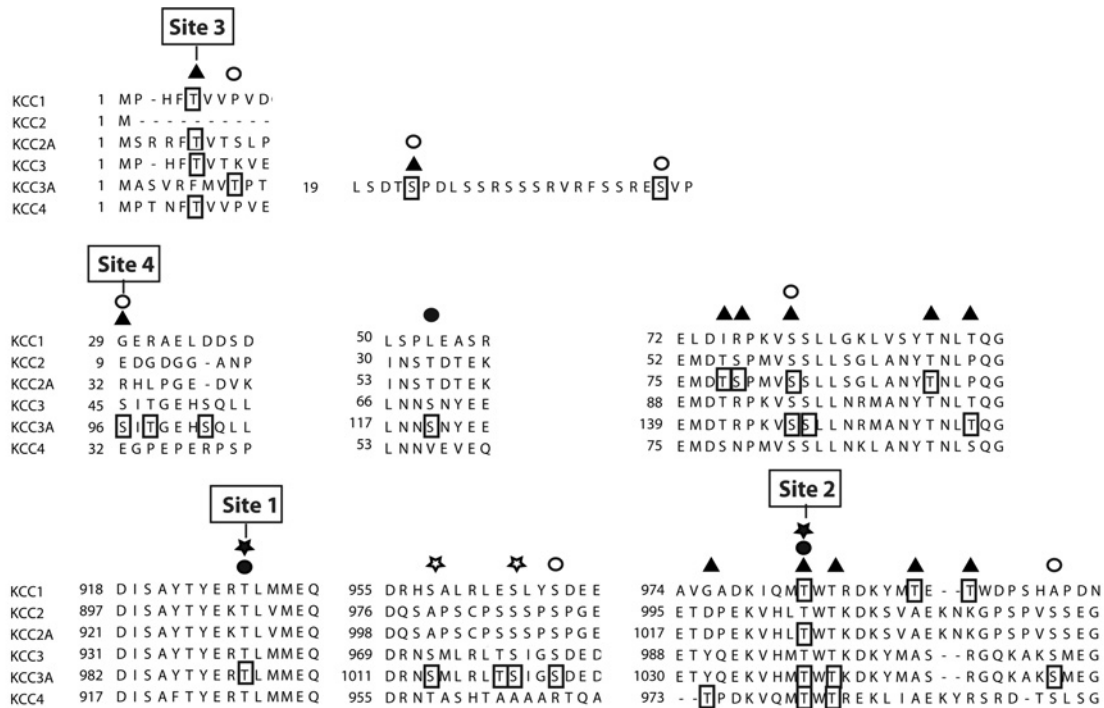
ES cells were plated in 12-well plates (2.4-cm diameter/well) and the <sup>86</sup>Rb<sup>+</sup>-uptake assay was performed on cells that were 80% confluent. HEK-293 cells were plated at a confluence of 50–60% in 12-well plates (2.4-cm diameter per/well) and transfected with wild-type or various mutant forms of full-length FLAG-tagged human KCCs. Each well of HEK-293 cells was transfected with 2.5  $\mu\text{l}$  of 1 mg/ml polyethylenimine and 1  $\mu\text{g}$  of plasmid DNA. The <sup>86</sup>Rb<sup>+</sup>-uptake assay was performed on the cells at 36 h post-transfection. In both cases, culture medium was removed from the wells and replaced with either isotonic or hypotonic medium for 15 min at 37°C. Cell medium was removed by means of aspiration with a vacuum pump and replaced with stimulating medium plus inhibitors including 1 mM ouabain and

0.1 mM bumetanide, to prevent <sup>86</sup>Rb<sup>+</sup> uptake via NKCC1, for a further 15 min. After this period, the medium was removed and replaced with isotonic medium plus inhibitors containing 2  $\mu\text{Ci/ml}$  <sup>86</sup>Rb<sup>+</sup> for 10 min at 37°C. After this incubation period, cells were rapidly washed three times with the respective ice-cold non-radioactive medium. The cells were lysed in 300  $\mu\text{l}$  of ice-cold lysis buffer and <sup>86</sup>Rb<sup>+</sup>-uptake tracer activity was quantified on a PerkinElmer liquid scintillation analyser.

## RESULTS

### SPAK and OSR1 complexed to MO25 $\alpha$ phosphorylate multiple KCC isoforms

KCC isoforms comprise a NTD and a CTD separated by a central 12 transmembrane region. We expressed the isolated NTD and CTD of KCC1, KCC2A, KCC3A and KCC4 in *E. coli* cells and tested whether these fragments could be phosphorylated by SPAK *in vitro*. Phosphorylation reactions were undertaken in the presence or absence of MO25 $\alpha$ , the SPAK/OSR1 regulatory subunit, which increases SPAK/OSR1 activity >100-fold [25]. Experiments revealed that SPAK phosphorylated the NTD and CTD of all four KCC isoforms tested in the presence, but not in the absence, of MO25 $\alpha$  (Figure 1A). Consistent with phosphorylation



□ Indication of a phosphorylation site marked in this study in Table 1, Table 2 and Table 3

▲ *In vitro* SPAK phosphorylation sites identified in Table 1 and Table 2

● *In vivo* KCC3A phosphorylation sites identified in this study that are dephosphorylated after hypotonic high potassium exposure (Table 3)

○ *In vivo* KCC3A phosphorylation sites identified in this study that are not significantly dephosphorylated after hypotonic high potassium exposure (Table 3)

★ KCC3A phosphorylation sites reported previously to be dephosphorylated after hypotonic high potassium exposure [42]

☆ KCC3A phosphorylation sites reported previously showing no change/regulation after hypotonic high potassium exposure [42]

## Figure 2 Conserved and unique identified regulatory phospho-sites in KCC isoforms

Sequence alignment of KCC1, KCC2, KCC2A, KCC3, KCC3A and KCC4 isoforms that show the position of the *in vitro* and *in vivo* phosphorylation sites identified in the present study (boxed residues). Boxed residues are phosphorylation sites that are listed in Tables 1–3. ▲, *in vitro* phosphorylation sites listed in Tables 1 and 2. ●, *in vivo* KCC3A phosphorylation sites that are dephosphorylated following exposure of cells to hypotonic high  $K^+$  conditions listed in Table 3. ○, *in vivo* KCC3A phosphorylation sites that are not influenced by exposure of cells to hypotonic high  $K^+$  conditions listed in Table 3. ★, *in vivo* KCC3A phosphorylation sites that were identified by the Lifton group [42] to become dephosphorylated following exposure of cells to hypotonic high  $K^+$  conditions. ☆, *in vivo* KCC3A phosphorylation sites that were previously identified [42] and not influenced by hypotonic high  $K^+$  conditions. It should be noted that as all experiments were done with the shorter KCC3A splice variant that lacks nine amino acid N-terminal residues, in order to be consistent with most previous literature studies, numbering of residues for KCC3A is based on the nine-residue-longer KCC3 variant.

of KCC fragments being mediated specifically by SPAK, the kinase-dead SPAK [D212A] mutant failed to phosphorylate KCC isoforms in the presence of MO25 $\alpha$  (Figure 1B). OSR1, in the presence, but not absence, of MO25 $\alpha$ , also phosphorylated the NTD and CTD of all KCC isoforms (Figure 1C). In contrast, kinase-dead OSR1 [D164A] failed to phosphorylate all KCC isoforms (Figure 1D). These data demonstrate that both SPAK and OSR1 are capable of phosphorylating the NTD and CTD of multiple KCC isoforms when complexed with MO25 $\alpha$ .

### Identification of *in vitro* SPAK/OSR1 phosphorylation sites

To map the sites that the SPAK–MO25 $\alpha$  complex phosphorylates on KCC isoforms, we performed phosphorylation reactions in the presence of radioactive [ $\gamma$ - $^{32}$ P]ATP, and then digested them with trypsin. The resulting  $^{32}$ P-labelled tryptic peptides were isolated by HPLC and the identity and site of phosphorylation was determined by employing a combination of MS and solid-phase Edman sequencing (Figure 2, and Tables 1 and 2). We also analysed directly the phosphorylation reactions using orbitrap MS analysis to pinpoint residues phosphorylated by SPAK–MO25 $\alpha$  (Figure 2 and Table 1).

Notably, the SPAK–MO25 $\alpha$  complex was found to phosphorylate all KCC isoforms at the critical Site-2 (Thr<sup>983</sup> in KCC1, Thr<sup>1030</sup> in KCC2A, Thr<sup>1048</sup> in KCC3A and Thr<sup>980</sup> in KCC4; Figure 2 and Table 1). SPAK–MO25 $\alpha$  also phosphorylated KCC1, KCC2A and KCC4 at a conserved N-terminal threonine residue that we have termed Site-3 (Thr<sup>5</sup> in KCC1 and Thr<sup>6</sup> in KCC2A/KCC4; Figure 2). Site-3 is not conserved in the KCC3A splice variant employed, but is conserved in the KCC3 splice variant (Thr<sup>5</sup>) (Figure 2). Consistent with previous findings [51], SPAK–MO25 $\alpha$  also phosphorylated KCC3A at Ser<sup>96</sup> (Site-4) within a motif not present in other KCCs (Figure 2). Our analysis also revealed a limited number of other phosphorylation sites observed in only single isoforms, which have not been further investigated (Table 2). Importantly, we did not observe phosphorylation of the critical Site-1 residues by SPAK–MO25 $\alpha$  in any of the KCC isoforms tested.

### Mapping of KCC3A phosphorylation sites *in vivo*

We used MS orbitrap analysis of KCC3A transiently expressed in HEK-293 cells that were stimulated with either hypotonic low  $Cl^-$  conditions (where phosphorylation of Site-1 and

**Table 3** *In vivo* KCC3A phosphorylation sites identified in the present study

N-terminal FLAG-tagged KCC3A was overexpressed in HEK-293 cells. At 36 h post-transfection, cells were treated with either hypotonic low Cl<sup>–</sup> or hypotonic high K<sup>+</sup> conditions to induce dephosphorylation and hence activation of the KCC3A isoform for 30 min. KCC3A was immunoprecipitated and after electrophoresis on a polyacrylamide gel and Colloidal Blue staining, the bands corresponding to KCC3A were excised and digested with trypsin. Phosphorylated peptides were identified by combined MS and MS/MS analysis. The data was searched using the Mascot search algorithm run on a local server. The deduced amino acid sequence of each peptide is shown and the phosphorylated residue, where identified, is underlined and in bold font. The ratios of the abundance of each phosphopeptide that was detected in hypotonic high K<sup>+</sup> samples compared with the hypotonic low Cl<sup>–</sup> conditions was calculated using Xcalibur software. Lower case m indicates oxidized methionine. The conservation and location of each phosphorylated residue is illustrated in Figure 2. It should be noted that although experiments were done with the shorter KCC3A splice variant that lacks nine N-terminal residues, in order to be consistent with most previous literature studies, the numbering of residues is based on the nine-residue-longer KCC3 variant.

Phosphopeptide	MS (orbitrap)		Phosphorylation site	Xcalibur ratio (hypotonic low Cl <sup>–</sup> /hypotonic high K <sup>+</sup> )
	Mascot score (hypotonic high K <sup>+</sup> )	m/z (observed)		
<b>T</b> LMMEQR	39	494.70	Thr <sup>991</sup> (Site-1)	> 10-fold
VHM <b>T</b> WTK	31	491.71	Thr <sup>1048</sup> (Site-2)	> 10-fold
NAYLN <b>S</b> NYEEGDEYFDKNLALFEEEmDTRPK	75	1318.89	Ser <sup>129</sup>	No significant change
FMVTP <b>T</b> KIDDIPGLSD <b>T</b> SPDLSSR	87	891.42	Ser <sup>32</sup>	No significant change
IDDIPGLSD <b>T</b> SPDLSSR	74	934.42	Ser <sup>32</sup>	No significant change
FSSRE <b>S</b> VPETSR	31	487.88	Ser <sup>50</sup>	No significant change
TSH <b>P</b> QDVIEDLSQ <b>S</b> ITGEHSQLLDDGHKK	39	852.90	Ser <sup>96</sup> (Site 4)	No significant change
V <b>S</b> LLNR	41	434.71	Ser <sup>148</sup>	No significant change
L <b>T</b> SIG <b>S</b> DEDEETETYQEK	92	1077.44	Ser <sup>1032</sup>	No significant change
AK <b>S</b> MEGFQDLLNMRPDQSNVR	47	839.38	Ser <sup>1064</sup>	No significant change

Site-2 should be maximal) or hypotonic high K<sup>+</sup> conditions (which should induce dephosphorylation of Site-1 and Site-2), to map further KCC3A phosphorylation sites *in vivo* [42]. This confirmed that hypotonic high K<sup>+</sup> conditions did indeed induce a >10-fold reduction in phosphorylation of Site-1 (Thr<sup>991</sup>) and Site-2 (Thr<sup>1048</sup>) (Figure 2 and Table 3). Our analysis identified a number of other phosphorylated residues on KCC3A whose phosphorylation was not inhibited significantly by hypotonic conditions (Figure 2 and Table 3). Several of these sites have also been identified previously [42] (Figure 2).

### Creation and characterization of phospho-specific KCC antibodies

To develop a tool that is able to monitor the phosphorylation state of these critical KCC phospho-residues in cells and tissues, we raised phospho-specific antibodies that recognize the critical regulatory Site-1 (Thr<sup>991</sup>), Site-2 (Thr<sup>1048</sup>) or Site-4 (Ser<sup>96</sup>) residues in KCC3A. The antibodies recognized by immunoblot or immunoprecipitation (Figure 3A) wild-type KCC3A overexpressed in HEK-293 cells, but not a mutant version of KCC3A in which the phosphorylated residue was changed to alanine. These antibodies confirm that treatment of HEK-293 cells with hypotonic high K<sup>+</sup> conditions for 30 min induces almost complete dephosphorylation of KCC3A at Site-1 (Thr<sup>991</sup>) and Site-2 (Thr<sup>1048</sup>) (Figure 3A). We observed that hypotonic high K<sup>+</sup> conditions induced a significantly more moderate dephosphorylation of Site-4 (Ser<sup>96</sup>) compared with Site-1 and Site-2 (Figure 3A). Individual mutation of Site-1 (Thr<sup>991</sup>), Site-2 (Thr<sup>1048</sup>) or Site-4 (Ser<sup>96</sup>) did not significantly affect the phosphorylation of the other sites (Figure 3A).

The residues surrounding Site-1 and Site-2 are almost identical in all KCC isoforms (Figure 2), indicating that the phospho-specific antibodies raised against these residues would probably detect the equivalent residues on other KCC isoforms. Indeed, immunoblot and immunoprecipitation analysis revealed that the KCC3A phospho-specific Site-1 and Site-2 antibodies readily detected KCC1, KCC2 and KCC4 (Figure 3B) overexpressed in HEK-293 cells grown in basic control isotonic medium, but to a lesser extent in cells treated with hypotonic high K<sup>+</sup> conditions that induce the dephosphorylation of these residues.

### Linking SPAK/OSR1 with KCC3A phosphorylation and transport activity

To determine whether activation of the SPAK/OSR1 pathway promotes phosphorylation of KCC3A at Site-2 and Site-4, the residues that are phosphorylated *in vitro* (Figure 2 and Table 1), we exposed HEK-293 cells to hypotonic low Cl<sup>–</sup> conditions that stimulate SPAK/OSR1 [4]. We monitored WNK1 phosphorylation at its activating T-loop residue (Ser<sup>382</sup>), SPAK/OSR1 phosphorylation at the residue phosphorylated by WNK1 (Ser<sup>373</sup>/Ser<sup>325</sup>) and NKCC1 phosphorylation at residues phosphorylated by SPAK/OSR1 (Thr<sup>203</sup>, Thr<sup>207</sup> and Thr<sup>212</sup>) over a 30 min time period (Figure 4A). These experiments revealed that within 5 min of exposing HEK-293 cells to hypotonic low Cl<sup>–</sup> conditions, an increase in the phosphorylation of WNK1, SPAK/OSR1 and NKCC1 was observed, which was maximal within 10 min and sustained for 30 min. Consistent with SPAK/OSR1 mediating the phosphorylation of KCC3A at Site-2 and Site-4, we observed an increased phosphorylation of these residues within 5–10 min of exposing HEK-293 cells to hypotonic low Cl<sup>–</sup> conditions, and this phosphorylation was sustained for at least 30 min. Exposure of HEK-293 cells to hypotonic low Cl<sup>–</sup> conditions also promoted the phosphorylation of KCC at Site-1 over a similar time course as for Site-2 and Site-4 (Figure 4A).

We next analysed KCC3A activity by measuring <sup>86</sup>Rb<sup>+</sup> uptake in isotonic or hypotonic low Cl<sup>–</sup> conditions (Figure 4B). As expected given that KCC3A is maximally phosphorylated following hypotonic low Cl<sup>–</sup> conditions, very low KCC3A activity was observed (Figure 4B). Individual mutation of either Site-1 or Site-2 to alanine moderately activated KCC3A, and these mutants were still significantly inhibited by hypotonic low Cl<sup>–</sup> conditions (Figure 4B). In contrast, a KCC3A mutant in which both Site-1 and Site-2 were mutated to alanine was highly active and not inhibited further by hypotonic low Cl<sup>–</sup> conditions, thereby confirming that these are indeed the essential inhibitory sites.

We also treated HEK-293 cells with hypotonic high K<sup>+</sup> conditions to induce dephosphorylation of KCC3A. Time course analysis revealed that the most pronounced dephosphorylation of Site-1, Site-2 and Site-4 occurred within 15–30 min. Levels of WNK1, SPAK/OSR1 and NKCC1 phosphorylation were also reduced markedly after a 15–30 min exposure to hypotonic high K<sup>+</sup> conditions (Figure 4C). We then analysed KCC3A

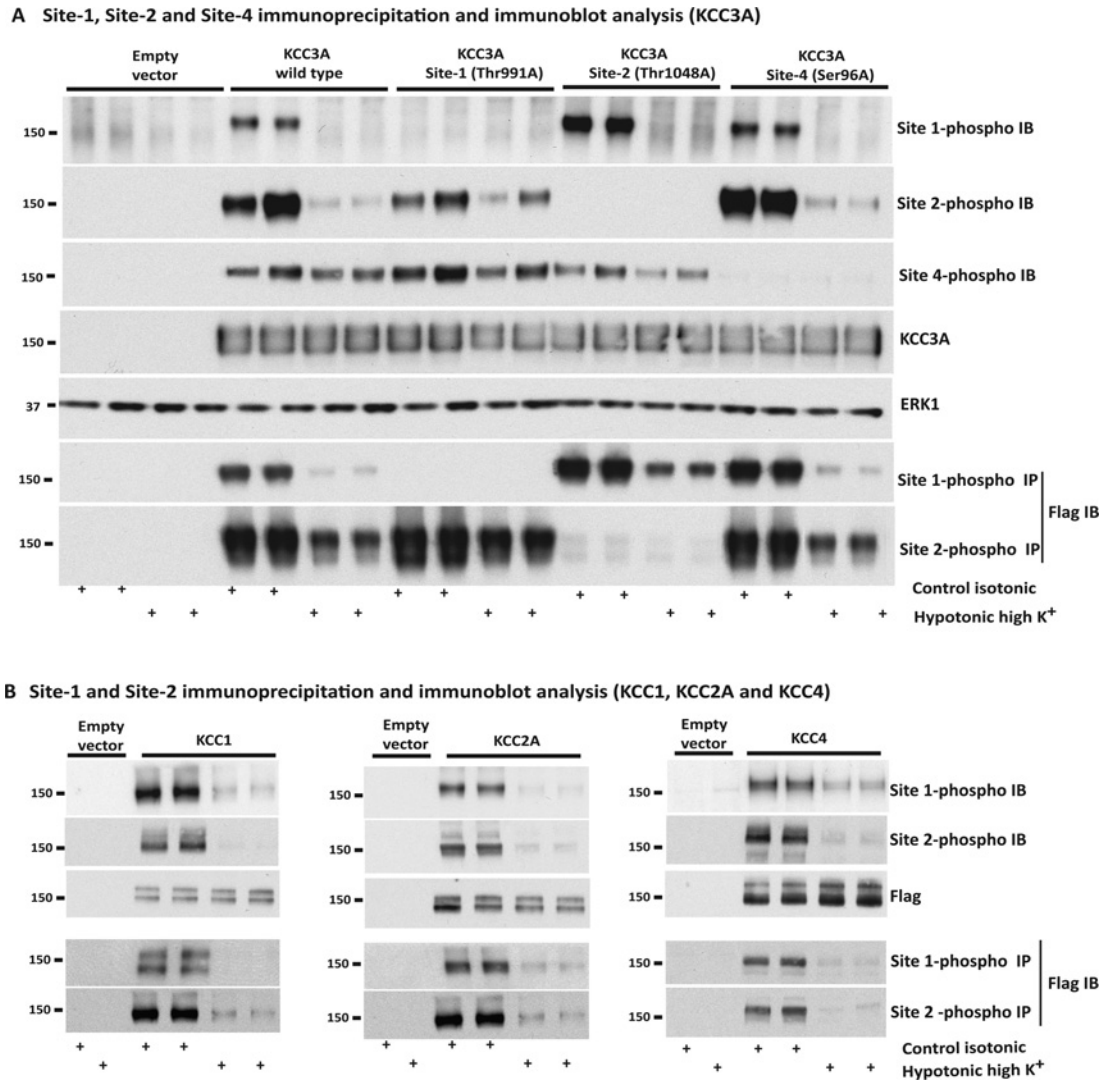


**Figure 3 Characterization of phospho-specific KCC Site-1, Site-2 and Site-4 antibodies**

(A) HEK-293 cells were transfected with constructs encoding a FLAG empty vector or the indicated wild-type or mutant constructs of N-terminal FLAG epitope-tagged KCC3A. At 36 h post-transfection, cells were treated with either basic control isotonic or hypotonic high  $K^+$  conditions to induce dephosphorylation of KCC3A for 30 min, and were then lysed. Total cell extracts were subjected to immunoblot (IB) analysis with the indicated phospho-specific antibodies raised against KCC3A Site-1 (pThr<sup>991</sup>), KCC3A Site-2 (pThr<sup>1048</sup>) and KCC3A Site-4 (pSer<sup>96</sup>), as well as total anti-KCC3A and anti-ERK1 antibodies (upper panels). The lysates were also subjected to immunoprecipitation (IP) with the indicated KCC3A phospho-antibodies, and immunoprecipitates were subjected to immunoblot analysis employing an anti-FLAG antibody. Similar results were obtained in three separate experiments. (B) Treatment as above, except cells were transfected with constructs encoding N-terminal FLAG-tagged versions of KCC1, KCC2A and KCC4. Solid lines indicates blots that were run on different gels. Molecular masses are all indicated in kDa on the left-hand side of the Western blots.

activity by measuring  $^{86}Rb^+$  uptake in isotonic or hypotonic high  $K^+$  conditions (Figure 4D). As expected, hypotonic high  $K^+$  conditions induced a marked activation of wild-type KCC3A (Figure 4D, upper panel). This was associated with a significant dephosphorylation of KCC3A Site-1 and Site-2 and a marked reduction in WNK1, SPAK/OSR1 and NKCC1 phosphorylation (Figure 4D, lower panel). Individual alanine mutation of Site-1 and Site-2, preventing phosphorylation at these sites, led to a moderate activation of KCC3A under isotonic conditions, and the activity of these mutants was stimulated further following exposure to hypotonic high  $K^+$  conditions. Mutation of both Site-1 and Site-2, as reported previously [52], resulted in constitutive activation of KCC3A that was not activated further by hypotonic high  $K^+$  conditions. Individual mutation of Site-4 was found to have no significant effect on KCC3A activity in isotonic

or hypotonic high  $K^+$  conditions (Figure 4D, upper panel), as reported previously [51].

#### Pharmacological evidence that SPAK/OSR1 directly phosphorylate KCC3A Site-2 and Site-4

A small molecule compound termed STOCK1S-50699 has recently been described that binds the CCT domain of SPAK/OSR1, thereby preventing WNK-mediated activation of the SPAK/OSR1, and consequently functioning as a WNK-SPAK/OSR1 inhibitor [30]. To obtain further evidence that SPAK/OSR1 regulate KCC3A phosphorylation, we exposed HEK-293 cells for 30 min to either basic control isotonic conditions or hypotonic low  $Cl^-$  (to activate SPAK/OSR1), and then treated the cells in the same conditions with increasing doses



of STOCK1S-50699 for an additional 30 min. These experiments confirmed that 1–10  $\mu\text{M}$  STOCK1S-50699 inhibited markedly, in a dose-dependent manner, SPAK/OSR1 phosphorylation at Ser<sup>373</sup>/Ser<sup>325</sup> (i.e. the activating site phosphorylated by WNK1) and NKCC1 phosphorylation at Thr<sup>203</sup>/Thr<sup>207</sup>/Thr<sup>212</sup> (SPAK/OSR1 sites whose phosphorylation is required for maximal transporter activity) in both hypotonic low Cl<sup>-</sup> conditions, as well as basic control isotonic conditions (Figure 5). These effects were paralleled by a similar suppression of KCC3A Site-2 (Thr<sup>1048</sup>) and Site-4 (Ser<sup>96</sup>) phosphorylation, consistent with the phosphorylation of these residues being mediated by SPAK/OSR1. Phosphorylation of Site-1 was also inhibited by STOCK1S-50699, but to a lower extent than Site-2 (Figure 5).

Consistent with STOCK1S-50699 promoting dephosphorylation of Site-2, in <sup>86</sup>Rb<sup>+</sup> uptake activity assays we observed that this inhibitor at concentrations over 3  $\mu\text{M}$  stimulated <sup>86</sup>Rb<sup>+</sup> uptake even under hypotonic low chloride conditions (Figure 5, upper panel). STOCK1S-50699 also stimulated <sup>86</sup>Rb<sup>+</sup> uptake under control isotonic conditions (Figure 5, upper panel).

#### Evidence that SPAK/OSR1 regulate the endogenous phosphorylation and activity of KCC2A, KCC3A and KCC4

To investigate how the lack of SPAK and OSR1 activity affects endogenous KCC isoform phosphorylation, we utilized previously described wild-type and double OSR1<sup>185A/185A</sup>/SPAK<sup>243A/243A</sup> knockin ES cells, in which the T-loop phosphorylation site on SPAK and OSR1, that is phosphorylated by WNK isoforms, is mutated to alanine to prevent their activating phosphorylation [29]. Wild-type and knockin cells were treated with basic control isotonic or hypotonic high K<sup>+</sup> conditions for 30 min to induce dephosphorylation of KCC isoforms, and then the harvested lysates were subjected to immunoprecipitation with Site-1 and Site-2 phospho-specific antibodies that immunoprecipitate all KCC isoforms when phosphorylated at these residues (Figure 3). The immunoprecipitates were then immunoblotted with antibodies that specifically recognize different individual KCC isoforms. In wild-type ES cells, endogenous KCC2A, KCC3A and KCC4 were phosphorylated at Site-1 and Site-2, as these co-transporters could readily be immunoprecipitated with the Site-1 and Site-2 phospho-specific antibodies (Figure 6, lower panel). As expected, immunoprecipitation of KCC2A, KCC3A and KCC4 isoforms was inhibited when wild-type ES cells were treated with hypotonic high K<sup>+</sup> conditions to induce dephosphorylation of these residues. In the OSR1<sup>185A/185A</sup>/SPAK<sup>243A/243A</sup> knockin ES cells, we still observed that endogenous KCC2A, KCC3A and KCC4 were phosphorylated at Site-1 to a similar extent as wild-type cells; however, consistent with SPAK/OSR1 predominately phosphorylating Site-2, Site-2 phosphorylation in endogenous KCC2A, KCC3A and KCC4 was abolished in knockin ES cells lacking SPAK/OSR1 activity (Figure 6, lower panel).

We then analysed endogenous KCCs activity in the OSR1<sup>185A/185A</sup>/SPAK<sup>243A/243A</sup> knockin ES cells by measuring <sup>86</sup>Rb<sup>+</sup>

uptake under basic control isotonic or hypotonic high K<sup>+</sup> conditions, and compared these results with wild-type ES cells. As expected, exposure of wild-type ES cells to hypotonic high K<sup>+</sup> conditions induced a significant ~2-fold activation of <sup>86</sup>Rb<sup>+</sup> uptake (Figure 6, upper panel), consistent with KCC activation. In contrast, in the double OSR1<sup>185A/185A</sup>/SPAK<sup>243A/243A</sup> knockin cells that lack SPAK/OSR1 activity, we observed an elevated basal activity of <sup>86</sup>Rb<sup>+</sup> uptake that was not stimulated markedly further by hypotonic high K<sup>+</sup> conditions, suggesting an increase in KCC activity secondary to decreased phosphorylation at Site-2 (Figure 6, upper panel). Together, these data provide evidence that endogenous silencing SPAK/OSR1 kinase activity is able to stimulate KCC activity by preventing Site-2 inhibitory phosphorylation.

We also investigated whether the SPAK/OSR1 inhibitor STOCK1S-50699 would affect the phosphorylation of endogenous KCC isoforms in either ES cells (Figure 7A) or HEK-293 cells (Figure 7B). These studies revealed that in both ES cells and HEK-293 cells treated under either basic isotonic or hypotonic low chloride conditions, STOCK1S-50699 inhibited the phosphorylation of KCC3a (ES and HEK-293) and KCC2a (ES) at Site-2 and Site-4, but not Site-1 (Figure 7).

#### DISCUSSION

The results of the present study reveal a major direct role for the WNK-regulated SPAK/OSR1 protein kinases in the regulation of KCC phosphorylation and function. Our data provide the first biochemical (Figure 1 and Table 1), pharmacological (Figure 5) and genetic (Figure 6) evidence that SPAK/OSR1 phosphorylates directly all KCC isoforms at the critical regulatory Site-2 residue (Thr<sup>1048</sup> in KCC3A) [42]. We also confirmed that SPAK/OSR1 phosphorylates directly a previously defined KCC3A-specific residue termed Site-4 (Ser<sup>96</sup>) [51]. Although the dephosphorylation of Site-1 and Site-2 plays the most important role in activating KCC isoforms [42], recent work has shown that dephosphorylation of Site-4 is also required for maximal KCC3A activation [51]. In addition to the finding that SPAK/OSR1 phosphorylates directly residues known to critically inhibit KCC function (Site-2 and Site-4), we have identified a novel N-terminal phosphorylation site (Site-3) present in all KCC isoforms except KCC3A (Thr<sup>5</sup> in KCC1/KCC3 and Thr<sup>6</sup> in KCC2A/KCC4) that is also phosphorylated directly by SPAK/OSR1 (Figure 2 and Table 1). Together, these data unambiguously define WNK-regulated SPAK/OSR1 as key regulators of KCC activity via direct inhibitory phosphorylation at multiple critical residues.

Our findings indicate that the MO25 $\alpha$  subunit is required for efficient phosphorylation of KCC isoforms by SPAK/OSR1, at least *in vitro* (Figure 1). This is consistent with MO25 $\alpha$  playing an essential role in stabilizing WNK-phosphorylated SPAK/OSR1 in an active conformation that can then efficiently phosphorylate its substrates [25]. These data emphasize the importance of including the MO25 $\alpha$  subunit in future studies for identification

#### Figure 4 SPAK/OSR1 kinase activity correlates with KCC3A phosphorylation status and KCC3A transport activity

(A and C) HEK-293 cells were transfected with constructs encoding wild-type N-terminal FLAG epitope-tagged KCC3A. At 36 h post-transfection, cells were treated for the indicated times with hypotonic low Cl<sup>-</sup> conditions (to activate SPAK/OSR1 pathway) (A) or hypotonic high K<sup>+</sup> conditions (to induce dephosphorylation of KCC3A) (C). Cells were immediately lysed and cell extracts were subjected to immunoblot (IB) and analysis with the indicated total and phospho-specific antibodies. (B and D) As above, except that the wild-type and the indicated mutant of KCC3A species were transfected into HEK-293 cells. Mutations are at: Site-1 (KCC3A [T991A]), Site-2 (KCC3A [T1048A]) and Site-4 (KCC3A [S96A]). At 36 h post-transfection, cells were treated for 30 min with either hypotonic low Cl<sup>-</sup> conditions (B) or hypotonic high K<sup>+</sup> conditions (D). <sup>86</sup>Rb<sup>+</sup> uptake was measured in the presence of 1 mM ouabain (inhibitor of the plasma membrane Na<sup>+</sup>/K<sup>+</sup>-ATPase sodium pump) and 0.1 mM bumetanide (inhibitor of NKCC1) in the uptake medium (for details, see the Materials and methods section). <sup>86</sup>Rb<sup>+</sup> uptake assays were then carried out over a 10 min period and was then quantified by scintillation counting. <sup>86</sup>Rb<sup>+</sup> uptake c.p.m. were normalized per mg of protein for each condition and plotted for both isotonic and hypotonic conditions. The results are presented as the means  $\pm$  S.D. <sup>86</sup>Rb<sup>+</sup> uptake for triplicate samples. Lysates were also subjected to immunoblot analysis with the indicated total and phospho-specific antibodies. Similar results were obtained in three separate experiments.

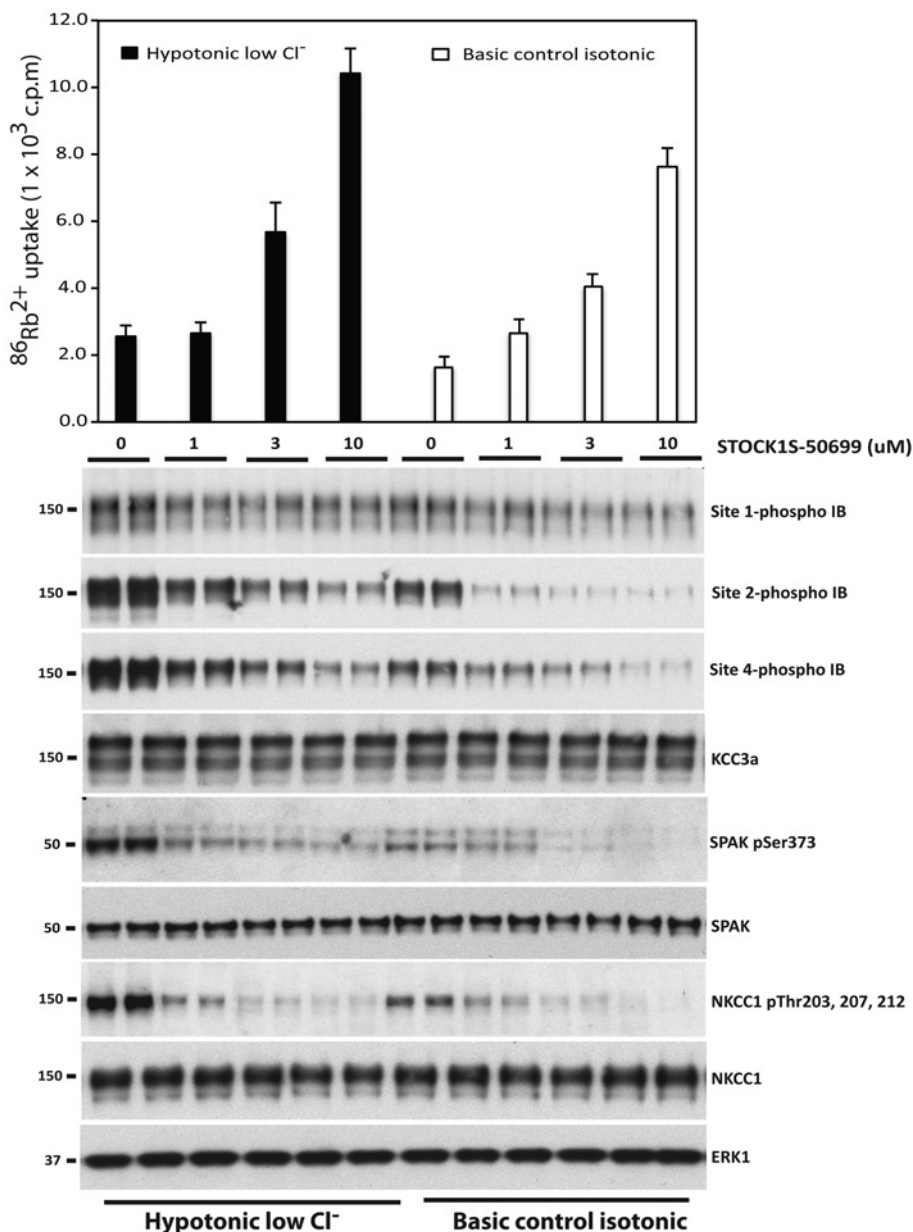


**Figure 5** The WNK-SPAK/OSR1 CCT domain inhibitor STOCK1S-50699 suppresses phosphorylation of KCC3A Site-2 and Site-4

HEK-293 cells were transfected with constructs encoding wild-type N-terminal FLAG epitope-tagged KCC3A. At 36 h post-transfection cells were exposed for 30 min to either basic control isotonic conditions or hypotonic low Cl<sup>-</sup> conditions (to activate the SPAK/OSR1 pathway), and then treated in the same conditions with the indicated doses of the SPAK/OSR1 CCT domain inhibitor STOCK1S-50699 [30] for an additional 30 min in the presence of 1 mM ouabain (an inhibitor of the plasma membrane Na<sup>+</sup>/K<sup>+</sup>-ATPase sodium pump) and 0.1 mM bumetanide (inhibitor of NKCC1). <sup>86</sup>Rb<sup>+</sup> uptake proceeded for 10 min and was then quantified by scintillation counting. <sup>86</sup>Rb<sup>+</sup> uptake c.p.m. values were normalized per mg of protein for each condition and plotted for both isotonic and hypotonic conditions. Cells were lysed and extracts were subjected to immunoblot analysis with the indicated total and phospho-specific antibodies (lower panel). Similar results were obtained in three separate experiments.

of novel SPAK/OSR1 substrates. Our conclusion that SPAK/OSR1 operate as key direct regulators of KCC isoforms is consistent with previous observations that found that knockdown of WNK1 expression, which would be expected to suppress SPAK/OSR1 activity, decreased phosphorylation of KCC3A at Site-2 (Thr<sup>1048</sup>) [42]. Similarly, the observation that overexpression of wild-type WNK3 (and WNK4), predicted to activate SPAK/OSR1, inhibits KCC isoforms in oocytes [39,40,43–45], but overexpression of a kinase-dead WNK3, predicted to inhibit SPAK/OSR1 in a dominant-negative mechanism, potentially activates KCC isoforms in oocytes [39], is

congruent with our conclusions that SPAK/OSR1, regulated by WNK kinase activity, play an important role in controlling KCC phosphorylation and activity.

Interestingly, our data suggest that SPAK/OSR1 may not phosphorylate directly the important Site-1 (Thr<sup>991</sup> in KCC3A) regulatory residue on KCC isoforms. The strongest and most direct evidence to support this conclusion is the finding that three endogenous KCC isoforms (KCC2, KCC3 and KCC4) are still phosphorylated on Site-1, but not on Site-2, in knockin ES cells that lack SPAK/OSR1 activity (Figure 6). Therefore, at least in ES cells that lack SPAK and OSR1 activity,

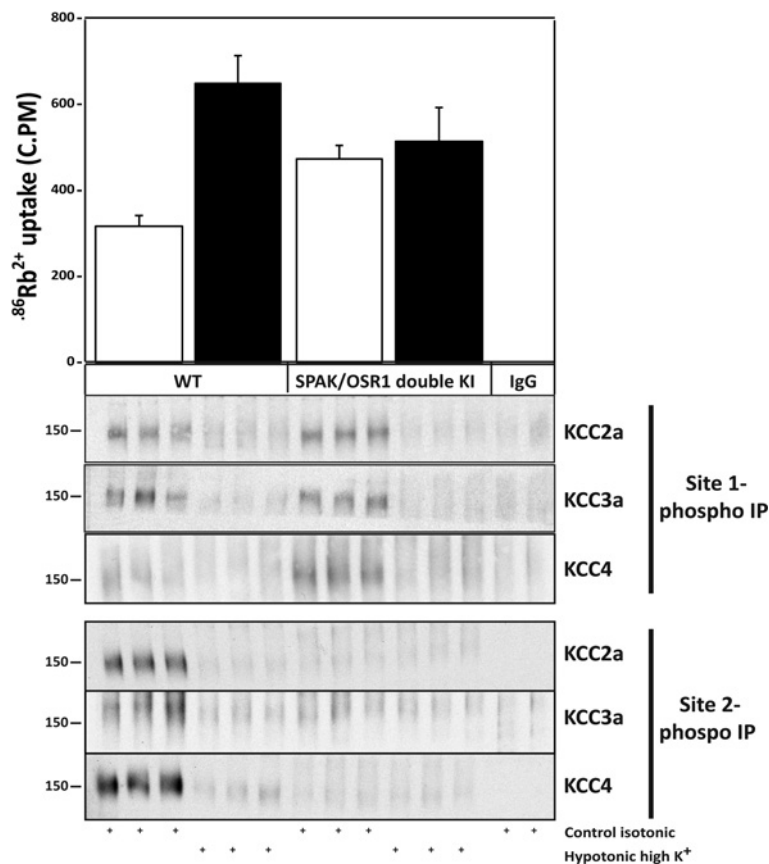


**Figure 6** WNK–SPAK/OSR1 regulation and phosphorylation of endogenous KCCs

Previously described matched wild-type and double OSR1<sup>185A/185A</sup>/SPAK<sup>243A/243A</sup> knockin ES cells [29], in which SPAK/OSR1 are inactive as the T-loop phosphorylation site that is phosphorylated by WNK isoforms is ablated, were incubated with either basic control isotonic medium (open bars) or hypotonic high K<sup>+</sup> medium (closed bars) for 30 min in the presence of 1 mM ouabain (an inhibitor of the plasma membrane Na<sup>+</sup>/K<sup>+</sup>-ATPase sodium pump) and 0.1 mM bumetanide (inhibitor of NKCC1). <sup>86</sup>Rb<sup>+</sup> uptake proceeded for 10 min and was then quantified by scintillation counting. <sup>86</sup>Rb<sup>+</sup> uptake c.p.m. values were normalized per mg of protein for each condition and plotted for both isotonic and hypotonic conditions. The lysates were also subjected to immunoprecipitation (IP) with the indicated KCC3A Site-1 and Site-2 phospho-antibodies that recognize all KCC isoforms (see Figure 3). The immunoprecipitates were then immunoblotted employing the indicated specific KCC isoform antibodies. Molecular masses are indicated in kDa on the left-hand side of the Western blots (lower panel). Similar results were obtained for three separate experiments.

another currently unknown kinase must exist that can efficiently phosphorylate Site-1. We also found that SPAK/OSR1 did not phosphorylate KCC isoforms at Site-1 *in vitro* (Figure 1 and Table 1). However, the finding that knockdown of WNK1 partially reduced phosphorylation of KCC3A at Site-1 [42], does suggest WNK isoforms regulate KCC phosphorylation at Site-1, either directly upstream of another kinase or perhaps via the regulation of a phosphatase. It would also appear that WNK1 itself does not directly phosphorylate Site-1, as we have also tested whether endogenously immunoprecipitated WNK1 is capable of phosphorylating Site-1 directly on isolated KCC fragments or full-length immunoprecipitated KCC3A. We found that under conditions that WNK1 efficiently phosphorylates catalytically inactive OSR1, no marked phosphorylation of Site-1 or Site-2 was observed when employing the phospho-specific antibodies as readouts for this activity (P. de los Heros, unpublished work). Further work is required to understand how WNK isoforms might control Site-1 phosphorylation and to what extent SPAK/OSR1 is involved. It may be that other WNK isoforms, such as WNK3, are directly involved in KCC Site-1 regulation, given the activating effects of kinase-dead WNK3 on KCCs *in vitro* [39]; this is one obvious candidate requiring further detailed biochemical examination. Also consistent with a role for the WNK–SPAK/OSR1 cascade regulating Site-1 phosphorylation,

we observed that the CCT domain inhibitor STOCK1S-50699 partially suppresses KCC3A Site-1 phosphorylation, albeit to a lesser extent than its inhibition of SPAK/OSR1 activity and KCC3A Site-2 phosphorylation (Figure 5). Notably, to check the selectivity of STOCK1S-50699, we assessed the effect of a high concentration of this inhibitor (10 μM) on the activity of 150 protein kinases *in vitro* and found that it does not significantly inhibit the activity of any other kinase, confirming that this compound is not a general protein kinase inhibitor (<http://www.kinase-screen.mrc.ac.uk/kinase-inhibitors>).

Our data emphasize that the phosphorylation of Site-1, Site-2 and Site-4 are co-ordinately regulated. For example, following exposure of cells to conditions that activate the WNK signalling pathway (hypotonic low Cl<sup>-</sup>), we observed a stimulation of phosphorylation of Site-1 and Site-2 of the KCCs, closely accompanied with increased phosphorylation of WNK1, SPAK/OSR1 and NKCC1 (Figure 4A). Conversely, exposure of cells to conditions that inhibit the WNK signalling network (hypotonic high K<sup>+</sup>) resulted in dephosphorylation of Site-1 and Site-2 in the KCCs, as well as WNK1, SPAK/OSR1 and NKCC1 (Figure 4C). One important unresolved question concerns the mechanism by which extracellular conditions, such as hypotonic high K<sup>+</sup>, are detected, and how this signal is transduced to trigger the dephosphorylation of WNK pathway components and KCC

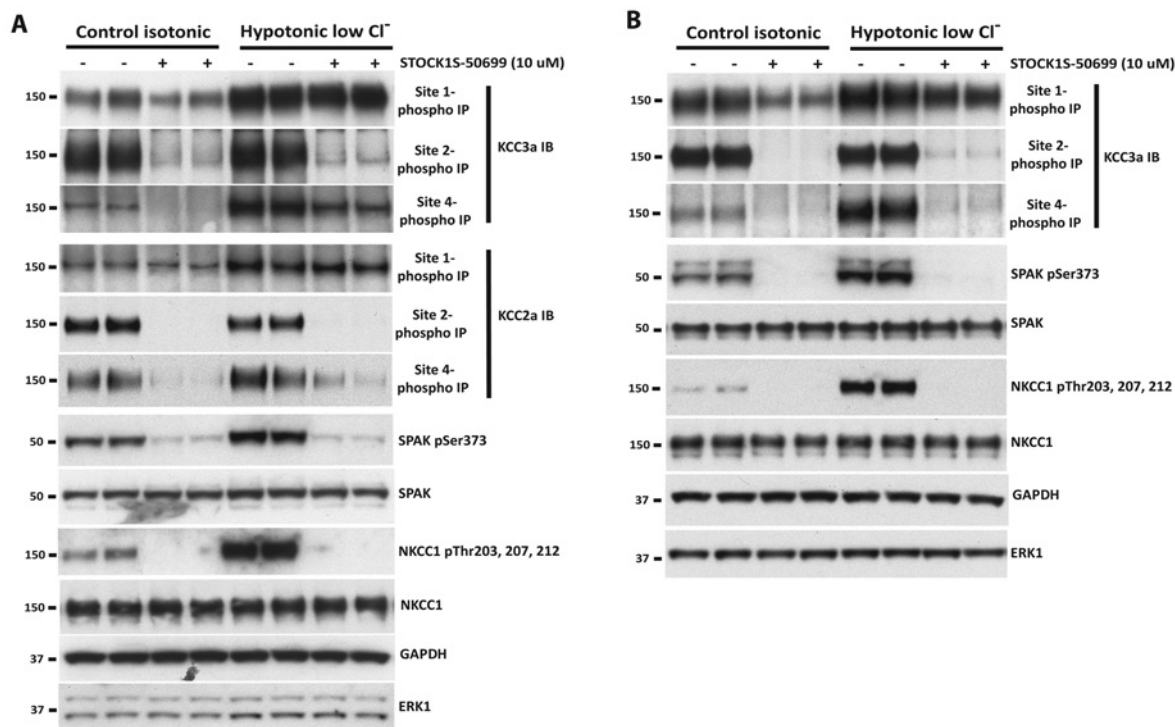


**Figure 7** STOCK1S-50699 inhibits phosphorylation of endogenous KCC isoforms at Site-2 and Site-4 in ES and HEK-293 cells

ES (A) or HEK-293 (B) cells were exposed for 30 min to either basic control isotonic conditions or hypotonic low  $Cl^-$  conditions (to activate the SPAK/OSR1 pathway), and then treated under the same conditions with the indicated doses of the SPAK/OSR1 CCT domain inhibitor STOCK1S-50699 [30] for an additional 30 min. The lysates were subjected to immunoprecipitation (IP) with the indicated KCC3A Site-1, Site-2 and Site-4 phospho-antibodies that recognize all KCC isoforms (see Figure 3). The immunoprecipitates were then immunoblotted (IB) employing the indicated specific KCC isoform antibodies. Cells lysates were also subjected to immunoblot analysis with the indicated total and phospho-specific antibodies. Similar results were obtained in three separate experiments. GAPDH, glyceraldehyde-3-phosphate dehydrogenase.

isoforms. Protein phosphatase(s) and their associated regulatory subunits that tether these enzymes to their targets are likely to play a critical role in this pathway, illustrated by the fact that all KCC isoforms, as well as core WNK pathway components, are robustly dephosphorylated within 15 min of exposure of cells to hypotonic high  $K^+$  conditions (Figure 4C). Several previous studies have highlighted that several general protein phosphatase inhibitors [40,53] block activation of KCC isoforms. Previous work has also implicated protein phosphatase-4 in the dephosphorylation of NCC at the critical Thr<sup>60</sup> regulated by the WNK-SPAK/OSR1 pathway [54]. In future studies, it would be important to determine the identity of the protein phosphatase catalytic activity, as well as the targeting regulatory subunit, that acts on the KCC isoforms, and to determine further whether the activity of this phosphatase complex is regulated by osmotic conditions. It would also be important to define whether the same or different protein phosphatase complexes act on different KCC isoforms and components of the WNK signalling system.

The importance of co-ordinating cellular  $Cl^-$  influx and efflux has long been appreciated [9,17]. The finding that SPAK/OSR1 kinases phosphorylate and thereby trigger activation of the  $Na^+$ -driven  $Cl^-$  influx co-transporters (NKCC1, NKCC2 and NCC) and also phosphorylate and inhibit  $K^+$ -driven  $Cl^-$  efflux co-transporters (KCC1, KCC2, KCC3 and KCC4), provides a simple mechanism to explain how these critical  $Na^+$  and  $K^+$  co-transporters are reciprocally and co-ordinately controlled (Figure 8). Stimuli such as hypotonic low  $Cl^-$  conditions that activate the WNK-SPAK/OSR1 pathway will induce net cellular  $Cl^-$  absorption by promoting phosphorylation, thereby activating the N[K]CCs and concurrently inhibiting the KCCs. In contrast,

stimuli that inactivate the WNK-SPAK/OSR1 pathway, such as hypotonic high  $K^+$  conditions, will suppress cellular  $Cl^-$  absorption by promoting dephosphorylation, thereby inhibiting the N[K]CCs and concurrently stimulating the KCCs. This co-ordinated and potent mechanism, with opposite effects on the main  $Cl^-$  influx and  $Cl^-$  efflux mediators involved in cellular  $Cl^-$  homeostasis, is of obvious interest for drug development. Our data suggest that this mechanism is druggable by the targeting of the CCT domain within SPAK/OSR1, which interferes with WNK activation. Given the anticipated net effects of WNK-SPAK/OSR1 signalling on increasing cellular  $Cl^-$  influx, we propose that the inhibition of this pathway with kinase inhibitors resembling STOCK1S-50699 might be a novel potent strategy to enhance cellular  $Cl^-$  extrusion. The phenotypes of human and mice with alterations in the WNK-SPAK/OSR1 pathway suggest that such a drug might be a novel  $K^+$ -sparing diuretic with special potency as an anti-hypertensive, since it would suppress renal salt re-absorption (and via effects on intravascular volume, blood pressure) in a more co-ordinated and balanced manner than thiazide and loop diuretics, which only suppress the activity of NCC (thiazide) or NKCC2 (loop diuretics) individually. Moreover, given the recent interest and proof of concept of small molecule enhancers of neuronal  $Cl^-$  extrusion via KCC2 activation to treat diseases featuring GABAergic (GABA is  $\gamma$ -aminobutyric acid) disinhibition secondary to impaired KCC2 activity [55,56], we propose that an especially potent way to enhance neuronal  $Cl^-$  extrusion would be to concurrently inhibit  $Cl^-$  influx via NKCC1 and activate  $Cl^-$  efflux via KCC2 [57]; our results suggest this could be done by inhibiting WNK-SPAK/OSR1 signalling. These hypotheses are testable, given the existence of a

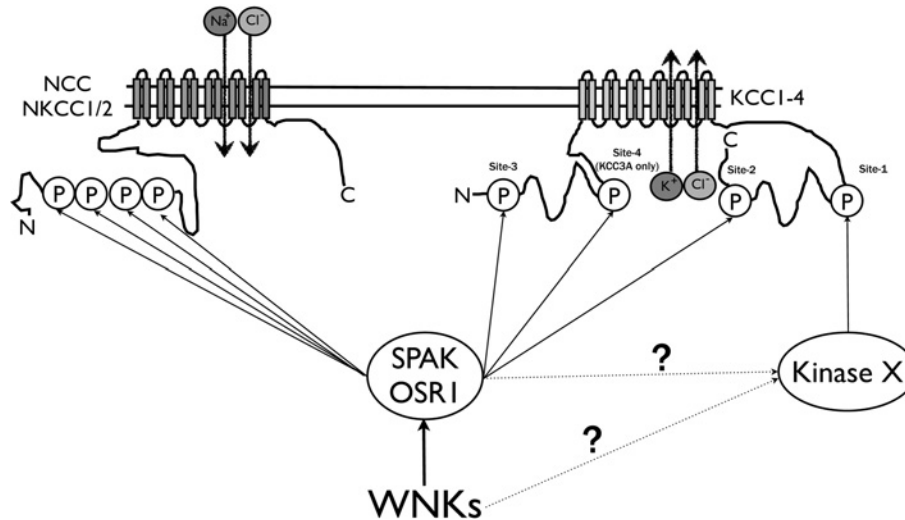


**Figure 8** Proposed mechanism of reciprocal regulation of the N[K]CC and KCC co-transporters by the WNK-SPAK/OSR1 cascade

SPAK/OSR1 are activated by WNK isoforms and then phosphorylate the NTD of the  $\text{Na}^+$ -driven CCCs (NKCC1, NKCC2 and NCC), thereby stimulating influx of  $\text{Cl}^-$  (and  $\text{Na}^+$ ). Work undertaken in the present study establishes that SPAK/OSR1 also phosphorylates  $\text{K}^+$ -driven CCCs (KCC1, KCC2, KCC3 and KCC4) at residues located in both their NTD and CTD, thereby stimulating efflux of  $\text{Cl}^-$  (and  $\text{K}^+$ ). Phosphorylation of Site-2 by SPAK/OSR1 greatly contributes to the regulation of the KCC activity. Site-1 phosphorylation also plays a major role in regulating KCC activity; the present study indicates that SPAK/OSR1 may not itself phosphorylate this site directly, but WNKs and/or SPAK/OSR1 may influence the activity of the kinase that phosphorylates Site-1. Further work is required to establish the roles that Site-3 phosphorylation within the NTD plays. Site-4 is only present in the KCC3 and KCC3A splice variants, and previous work suggests that phosphorylation at this site plays a minor role in regulating KCC activity [51].

WNK-SPAK/OSR1 inhibitor and phospho-specific antibody readouts of pathway activity, with potential implications for the therapeutic modulation of epithelial and neuronal ion transport.

#### AUTHOR CONTRIBUTION

Paola de los Heros and Jinwei Zhang undertook all of the experimental work. Robert Gourlay and David Campbell performed and analysed all MS. Maria Deak and Thomas Macartney generated all of the DNA plasmids. Paola de los Heros, Jinwei Zhang, Kristopher Kahle and Dario Alessi planned the experiments, analysed the data and wrote the paper.

#### ACKNOWLEDGEMENTS

We thank the excellent technical support of the MRC-Protein Phosphorylation and Ubiquitylation Unit (PPU) DNA Sequencing Service (co-ordinated by Nicholas Helps), the MRC-PPU tissue culture team (co-ordinated by Kirsten McLeod), and the Division of Signal Transduction Therapy (DSTT) antibody and protein purification teams (co-ordinated by Hilary McLauchlan and James Hastie).

#### FUNDING

This work was supported by the Medical Research Council and the Wellcome Trust [grant number 091415] as well as the pharmaceutical companies supporting the Division of Signal Transduction Therapy Unit (AstraZeneca, Boehringer-Ingelheim, GlaxoSmithKline, Merck KgaA, Janssen Pharmaceutica and Pfizer). K.T.K. is supported by the Manton Center for Orphan Diseases at Children's Hospital Boston at Harvard Medical School, and the Harvard/MIT Joint Research Grants Program in Basic Neuroscience.

#### REFERENCES

- Hoffmann, E. K., Lambert, I. H. and Pedersen, S. F. (2009) Physiology of cell volume regulation in vertebrates. *Physiol. Rev.* **89**, 193–277
- Arroyo, J. P., Kahle, K. T. and Gamba, G. (2013) The SLC12 family of electroneutral cation-coupled chloride cotransporters. *Mol. Aspects Med.* **34**, 288–298
- Moriguchi, T., Urushiyama, S., Hisamoto, N., Iemura, S., Uchida, S., Natsume, T., Matsumoto, K. and Shibuya, H. (2005) WNK1 regulates phosphorylation of cation-chloride-coupled cotransporters via the STE20-related kinases, SPAK and OSR1. *J. Biol. Chem.* **280**, 42685–42693
- Richardson, C., Rafiqi, F. H., Karlsson, H. K., Moleleki, N., Vandewalle, A., Campbell, D. G., Morrice, N. A. and Alessi, D. R. (2008) Activation of the thiazide-sensitive  $\text{Na}^+$ - $\text{Cl}^-$  cotransporter by the WNK-regulated kinases SPAK and OSR1. *J. Cell Sci.* **121**, 675–684
- Richardson, C., Sakamoto, K., de los Heros, P., Deak, M., Campbell, D. G., Prescott, A. R. and Alessi, D. R. (2011) Regulation of the NKCC2 ion cotransporter by SPAK-OSR1-dependent and -independent pathways. *J. Cell Sci.* **124**, 789–800
- Piechotta, K., Lu, J. and Delpire, E. (2002) Cation chloride cotransporters interact with the stress-related kinases Ste20-related proline-alanine-rich kinase (SPAK) and oxidative stress response 1 (OSR1). *J. Biol. Chem.* **277**, 50812–50819
- Dowd, B. F. and Forbush, B. (2003) PASK (proline-alanine-rich STE20-related kinase), a regulatory kinase of the Na-K-Cl cotransporter (NKCC1). *J. Biol. Chem.* **278**, 27347–27353
- Piechotta, K., Garbarini, N., England, R. and Delpire, E. (2003) Characterization of the interaction of the stress kinase SPAK with the  $\text{Na}^+$ - $\text{K}^+$ - $2\text{Cl}^-$  cotransporter in the nervous system: evidence for a scaffolding role of the kinase. *J. Biol. Chem.* **278**, 52848–52856
- Adragna, N. C., Di Fulvio, M. and Lauf, P. K. (2004) Regulation of K-Cl cotransport: from function to genes. *J. Biol. Chem.* **279**, 109–137
- Uvarov, P., Ludwig, A., Markkanen, M., Pruunsild, P., Kaila, K., Delpire, E., Timmusk, T., Rivera, C. and Airaksinen, M. S. (2007) A novel N-terminal isoform of the neuron-specific K-Cl cotransporter KCC2. *J. Biol. Chem.* **282**, 30570–30576
- Pearson, M. M., Lu, J., Mount, D. B. and Delpire, E. (2001) Localization of the  $\text{K}^+$ - $\text{Cl}^-$  cotransporter, KCC3, in the central and peripheral nervous systems: expression in the choroid plexus, large neurons and white matter tracts. *Neuroscience* **103**, 481–491
- Gagnon, K. B. and Delpire, E. (2013) Physiology of SLC12 transporters: lessons from inherited human genetic mutations and genetically engineered mouse knockouts. *Am. J. Physiol. Cell Physiol.* **304**, C693–C714
- Bernstein, P. L. and Ellison, D. H. (2011) Diuretics and salt transport along the nephron. *Semin. Nephrol.* **31**, 475–482
- Lytle, C., Xu, J. C., Biemesderfer, D., Haas, M. and Forbush, III, B. (1992) The Na-K-Cl cotransport protein of shark rectal gland. I. Development of monoclonal antibodies, immunofluorescence purification, and partial biochemical characterization. *J. Biol. Chem.* **267**, 25428–25437
- Jennings, M. L. and Schulz, R. K. (1991) Okadaic acid inhibition of K-Cl cotransport. Evidence that protein dephosphorylation is necessary for activation of transport by either cell swelling or N-ethylmaleimide. *J. Gen. Physiol.* **97**, 799–817
- Dunham, P. B., Stewart, G. W. and Ellory, J. C. (1980) Chloride-activated passive potassium transport in human erythrocytes. *Proc. Natl. Acad. Sci. U.S.A.* **77**, 1711–1715

- 17 Haas, M. and Forbush, III, B. (1998) The Na-K-Cl cotransporters. *J. Bioenerg. Biomembr.* **30**, 161–172
- 18 Gamba, G. (2005) Molecular physiology and pathophysiology of electroneutral cation-chloride cotransporters. *Physiol. Rev.* **85**, 423–493
- 19 Strange, K., Denton, J. and Nehrke, K. (2006) Ste20-type kinases: evolutionarily conserved regulators of ion transport and cell volume. *Physiology* **21**, 61–68
- 20 Kahle, K. T., Ring, A. M. and Lifton, R. P. (2008) Molecular physiology of the WNK kinases. *Annu. Rev. Physiol.* **70**, 329–355
- 21 Gagnon, K. B. and Delpire, E. (2012) Molecular physiology of SPAK and OSR1: two Ste20-related protein kinases regulating ion transport. *Physiol. Rev.* **92**, 1577–1617
- 22 Richardson, C. and Alessi, D. R. (2008) The regulation of salt transport and blood pressure by the WNK-SPAK/OSR1 signalling pathway. *J. Cell Sci.* **121**, 3293–3304
- 23 Vitari, A. C., Deak, M., Morrice, N. A. and Alessi, D. R. (2005) The WNK1 and WNK4 protein kinases that are mutated in Gordon's hypertension syndrome phosphorylate and activate SPAK and OSR1 protein kinases. *Biochem. J.* **391**, 17–24
- 24 Zagorska, A., Pozo-Guisado, E., Boudeau, J., Vitari, A. C., Rafiqi, F. H., Thastrup, J., Deak, M., Campbell, D. G., Morrice, N. A., Prescott, A. R. and Alessi, D. R. (2007) Regulation of activity and localization of the WNK1 protein kinase by hyperosmotic stress. *J. Cell Biol.* **176**, 89–100
- 25 Filippi, B. M., de los Heros, P., Mehellou, Y., Navratilova, I., Gourlay, R., Deak, M., Plater, L., Toth, R., Zeqiraj, E. and Alessi, D. R. (2011) MO25 is a master regulator of SPAK/OSR1 and MST3/MST4/YSK1 protein kinases. *EMBO J.* **30**, 1730–1741
- 26 Vitari, A. C., Thastrup, J., Rafiqi, F. H., Deak, M., Morrice, N. A., Karlsson, H. K. and Alessi, D. R. (2006) Functional interactions of the SPAK/OSR1 kinases with their upstream activator WNK1 and downstream substrate NKCC1. *Biochem. J.* **397**, 223–231
- 27 Delpire, E. and Gagnon, K. B. (2007) Genome-wide analysis of SPAK/OSR1 binding motifs. *Physiol. Genomics* **28**, 223–231
- 28 Villa, F., Deak, M., Alessi, D. R. and van Aalten, D. M. (2008) Structure of the OSR1 kinase, a hypertension drug target. *Proteins* **73**, 1082–1087
- 29 Thastrup, J. O., Rafiqi, F. H., Vitari, A. C., Pozo-Guisado, E., Deak, M., Mehellou, Y. and Alessi, D. R. (2012) SPAK/OSR1 regulate NKCC1 and WNK activity: analysis of WNK isoform interactions and activation by T-loop trans-autophosphorylation. *Biochem. J.* **441**, 325–337
- 30 Mori, T., Kikuchi, E., Watanabe, Y., Fujii, S., Ishigami-Yuasa, M., Kagechika, H., Sahara, E., Rai, T., Sasaki, S. and Uchida, S. (2013) Chemical library screening for WNK signalling inhibitors using fluorescence correlation spectroscopy. *Biochem. J.* **455**, 339–345
- 31 Lenertz, L. Y., Lee, B. H., Min, X., Xu, B. E., Wedin, K., Earnest, S., Goldsmith, E. J. and Cobb, M. H. (2005) Properties of WNK1 and implications for other family members. *J. Biol. Chem.* **280**, 26653–26658
- 32 Wilson, F. H., Disse-Nicodeme, S., Choate, K. A., Ishikawa, K., Nelson-Williams, C., Desitter, I., Gunel, M., Milford, D. V., Lipkin, G. W., Achard, J. M. et al. (2001) Human hypertension caused by mutations in WNK kinases. *Science* **293**, 1107–1112
- 33 Simon, D. B., Nelson-Williams, C., Bia, M. J., Ellison, D., Karet, F. E., Molina, A. M., Vaara, I., Iwata, F., Cushner, H. M., Koolen, M. et al. (1996) Gitelman's variant of Bartter's syndrome, inherited hypokalaemic alkalosis, is caused by mutations in the thiazide-sensitive Na-Cl cotransporter. *Nat. Genet.* **12**, 24–30
- 34 Simon, D. B., Karet, F. E., Hamdan, J. M., DiPietro, A., Sanjad, S. A. and Lifton, R. P. (1996) Bartter's syndrome, hypokalaemic alkalosis with hypercalciuria, is caused by mutations in the Na-K-2Cl cotransporter NKCC2. *Nat. Genet.* **13**, 183–188
- 35 Shao, L., Lang, Y., Wang, Y., Gao, Y., Zhang, W., Niu, H., Liu, S. and Chen, N. (2012) High-frequency variant p.T60M in NaCl cotransporter and blood pressure variability in Han Chinese. *Am. J. Nephrol.* **35**, 515–519
- 36 Yang, S. S., Lo, Y. F., Wu, C. C., Lin, S. W., Yeh, C. J., Chu, P., Sytwu, H. K., Uchida, S., Sasaki, S. and Lin, S. H. (2010) SPAK-knockout mice manifest Gitelman syndrome and impaired vasoconstriction. *J. Am. Soc. Nephrol.* **21**, 1868–1877
- 37 Rafiqi, F. H., Zuber, A. M., Glover, M., Richardson, C., Fleming, S., Jovanovic, S., Jovanovic, A., O'Shaughnessy, K. M. and Alessi, D. R. (2010) Role of the WNK-activated SPAK kinase in regulating blood pressure. *EMBO Mol. Med.* **2**, 63–75
- 38 Chiga, M., Rafiqi, F. H., Alessi, D. R., Sahara, E., Ohta, A., Rai, T., Sasaki, S. and Uchida, S. (2011) Phenotypes of pseudohypoadosteronism type II caused by the WNK4 D561A missense mutation are dependent on the WNK-OSR1/SPAK kinase cascade. *J. Cell Sci.* **124**, 1391–1395
- 39 Kahle, K. T., Rinehart, J., de Los Heros, P., Louvi, A., Meade, P., Vazquez, N., Hebert, S. C., Gamba, G., Gimenez, I. and Lifton, R. P. (2005) WNK3 modulates transport of Cl<sup>-</sup> in and out of cells: implications for control of cell volume and neuronal excitability. *Proc. Natl. Acad. Sci. U.S.A.* **102**, 16783–16788
- 40 de los Heros, P., Kahle, K. T., Rinehart, J., Bobadilla, N. A., Vazquez, N., San Cristobal, P., Mount, D. B., Lifton, R. P., Hebert, S. C. and Gamba, G. (2006) WNK3 bypasses the tonicity requirement for K-Cl cotransporter activation via a phosphatase-dependent pathway. *Proc. Natl. Acad. Sci. U.S.A.* **103**, 1976–1981
- 41 Gagnon, K. B., England, R. and Delpire, E. (2006) Volume sensitivity of cation-Cl<sup>-</sup> cotransporters is modulated by the interaction of two kinases: Ste20-related proline-alanine-rich kinase and WNK4. *Am. J. Physiol. Cell Physiol.* **290**, C134–C142
- 42 Rinehart, J., Maksimova, Y. D., Tanis, J. E., Stone, K. L., Hodson, C. A., Zhang, J., Risinger, M., Pan, W., Wu, D., Colangelo, C. M. et al. (2009) Sites of regulated phosphorylation that control K-Cl cotransporter activity. *Cell* **138**, 525–536
- 43 Cruz-Rangel, S., Gamba, G., Ramos-Mandujano, G. and Pasantes-Morales, H. (2012) Influence of WNK3 on intracellular chloride concentration and volume regulation in HEK293 cells. *Pflugers Arch.* **464**, 317–330
- 44 Cruz-Rangel, S., Melo, Z., Vazquez, N., Meade, P., Bobadilla, N. A., Pasantes-Morales, H., Gamba, G. and Mercado, A. (2011) Similar effects of all WNK3 variants on SLC12 cotransporters. *Am. J. Physiol. Cell Physiol.* **301**, C601–C608
- 45 Garzon-Muvdi, T., Pacheco-Alvarez, D., Gagnon, K. B., Vazquez, N., Ponce-Coria, J., Moreno, E., Delpire, E. and Gamba, G. (2007) WNK4 kinase is a negative regulator of K<sup>+</sup>-Cl<sup>-</sup> cotransporters. *Am. J. Physiol. Renal Physiol.* **292**, F1197–F1207
- 46 Durocher, Y., Perret, S. and Kamen, A. (2002) High-level and high-throughput recombinant protein production by transient transfection of suspension-growing human 293-EBNA1 cells. *Nucleic Acids Res.* **30**, E9
- 47 Woods, Y. L., Rena, G., Morrice, N., Barthel, A., Becker, W., Guo, S., Unterman, T. G. and Cohen, P. (2001) The kinase DYRK1A phosphorylates the transcription factor FKHR at Ser<sup>329</sup> *in vitro*, a novel *in vivo* phosphorylation site. *Biochem. J.* **355**, 597–607
- 48 Beullens, M., Vancauwenbergh, S., Morrice, N., Derua, R., Ceulemans, H., Waelkens, E. and Bollen, M. (2005) Substrate specificity and activity regulation of protein kinase MELK. *J. Biol. Chem.* **280**, 40003–40011
- 49 Campbell, D. G. and Morrice, N. A. (2002) Identification of protein phosphorylation sites by a combination of mass spectrometry and solid phase Edman sequencing. *J. Biomol. Tech.* **13**, 121–132
- 50 Williamson, B. L., Marchese, J. and Morrice, N. A. (2006) Automated identification and quantification of protein phosphorylation sites by LC/MS on a hybrid triple quadrupole linear ion trap mass spectrometer. *Mol. Cell. Proteomics* **5**, 337–346
- 51 Melo, Z., de los Heros, P., Cruz-Rangel, S., Vazquez, N., Bobadilla, N. A., Pasantes-Morales, H., Alessi, D. R., Mercado, A. and Gamba, G. (2013) N-terminal serine dephosphorylation is required for KCC3 cotransporter full activation by cell swelling. *J. Biol. Chem.* **288**, 31468–31476
- 52 Rinehart, J., Kahle, K. T., de Los Heros, P., Vazquez, N., Meade, P., Wilson, F. H., Hebert, S. C., Gimenez, I., Gamba, G. and Lifton, R. P. (2005) WNK3 kinase is a positive regulator of NKCC2 and NCC, renal cation-Cl<sup>-</sup> cotransporters required for normal blood pressure homeostasis. *Proc. Natl. Acad. Sci. U.S.A.* **102**, 16777–16782
- 53 Gusev, G. P. and Agalakova, N. I. (2010) Regulation of K-Cl cotransport in erythrocytes of frog *Rana temporaria* by commonly used protein kinase and protein phosphatase inhibitors. *J. Comp. Physiol. B Biochem. Syst. Environ. Physiol.* **180**, 385–391
- 54 Glover, M., Mercier Zuber, A., Figg, N. and O'Shaughnessy, K. M. (2010) The activity of the thiazide-sensitive Na<sup>+</sup>-Cl<sup>-</sup> cotransporter is regulated by protein phosphatase PP4. *Can. J. Physiol. Pharmacol.* **88**, 986–995
- 55 Gagnon, M., Bergeron, M. J., Lavertu, G., Castonguay, A., Tripathy, S., Bonin, R. P., Perez-Sanchez, J., Boudreau, D., Wang, B., Dumas, L. et al. (2013) Chloride extrusion enhancers as novel therapeutics for neurological diseases. *Nat. Med.* **19**, 1524–1528
- 56 Kahle, K. T., Staley, K. J., Nahed, B. V., Gamba, G., Hebert, S. C., Lifton, R. P. and Mount, D. B. (2008) Roles of the cation-chloride cotransporters in neurological disease. *Nat. Clin. Pract. Neurol.* **4**, 490–503
- 57 Kahle, K. T., Deeb, T. Z., Puskarjov, M., Silayeva, L., Liang, B., Kaila, K. and Moss, S. J. (2013) Modulation of neuronal activity by phosphorylation of the K-Cl cotransporter KCC2. *Trends Neurosci.* **36**, 726–737

Received 14 November 2013/19 December 2013; accepted 7 January 2014  
Published as BJ Immediate Publication 7 January 2014, doi:10.1042/BJ20131478